

Joint Statistics of Radio Frequency Interference in Multi-Antenna Receivers

Aditya Chopra, *Student Member, IEEE*, and Brian L. Evans, *Fellow, IEEE*

Abstract

Many wireless data communications systems, such as LTE, Wi-Fi and Wimax, have become or are rapidly becoming interference limited due to radio frequency interference (RFI) generated by both human-made and natural sources. Human-made sources of RFI include uncoordinated devices operating in the same frequency band, devices communicating in adjacent frequency bands, and computational platform subsystems radiating clock frequencies and their harmonics. Additive RFI for these wireless systems has predominantly non-Gaussian statistics, and is well modeled by the Middleton Class A distribution for centralized networks, and the symmetric alpha stable distribution for decentralized networks. Our primary contribution is the derivation of joint spatial statistical models of RFI generated from uncoordinated interfering sources randomly distributed around a multi-antenna receiver. The derivation is based on statistical-physical interference generation and propagation mechanisms. Prior results on joint statistics of multi-antenna interference model either spatially independent or spatially isotropic interference, and do not provide a statistical-physical derivation for certain network environments. Our proposed joint spatial statistical model captures a continuum between spatially independent and spatially isotropic statistics, and hence includes many previous results as special cases. Practical applications include co-channel interference modeling for various wireless network environments, including wireless *ad hoc*, cellular, local area, and femtocell networks.

Index Terms

Co-channel interference, Poisson point processes, impulsive noise, tail probability, spatial dependence.

A. Chopra and B. L. Evans are with the Wireless Networking and Communications Group, Department of Electrical and Computer Engineering, The University of Texas at Austin, TX, USA. E-mail: achopra@utexas.edu, bevans@ece.utexas.edu.

This research was supported by Intel Corporation.

I. INTRODUCTION

Wireless transceivers suffer degradation in communication performance due to radio frequency interference (RFI) generated by both human-made and natural sources. Human-made sources of RFI include uncoordinated wireless devices operating in the same frequency band (co-channel interference), devices communicating in adjacent frequency bands (adjacent channel interference), and computational platform subsystems radiating clock frequencies and their harmonics [1]. Dense spatial reuse of the available radio spectrum, required to meet increasing demand in user data rates also causes severe co-channel interference and may limit communication system performance. Network planning, resource allocation [2] and user scheduling [3] are strategies typically used to avoid RFI; however, these strategies are restricted to coordinated users operating over the same or co-existing communication standards [4]. Other RFI mitigation techniques include interference cancellation [5], interference alignment [6], and receiver back-off [7]; however, these too require some level of user or base station cooperation [8]. Furthermore, some level of uncoordinated residual interference is generally present in wireless receivers regardless of the interference cancellation strategy. Residual interference includes interference from uncoordinated users (out-of-cell interference in cellular networks and co-channel interference in *ad hoc* networks) or users in co-existing networks (interference from hotspots in femtocell networks).

Recent communication standards and research have focused on the use of multiple transmit and multiple receive antennas to increase data rate and communication reliability in wireless networks. Multi-antenna wireless receivers are increasingly being used in RFI-rich network environments. Accurate statistical models of RFI observed by multi-antenna receivers are needed in order to analyze communication performance of receivers [9], develop algorithms to mitigate the impact of RFI on communication performance [10], and improve network performance [11]. In this paper, we derive the joint statistics of RFI generated from a field of Poisson distributed interferers that are placed (i) over the entire plane, or (ii) outside of a interferer-free *guard zone* around the receiver.

Organization — Section II presents a concise survey of multi-dimensional statistical models of RFI. Section III discusses the system model of interference generation and propagation. The joint interference statistics are derived in Section IV. Section V discusses the impact of removing certain system model assumptions on RFI statistics. Section VI presents numerical simulations to corroborate our claims and the key takeaways are summarized in Section VII.

Notation — In this paper, scalar random variables are represented using upper-case notation or

Greek alphabet, random vectors are denoted using the boldface lower-case notation, and random matrices are denoted using the boldface upper-case notation. Deterministic parameters are represented using Greek alphabet, with the exception of N denoting the number of receive antennas. $\mathbb{E}_{\mathbf{X}}\{f(\mathbf{X})\}$ denotes the expectation of the function $f(\mathbf{X})$ with respect to the random variable \mathbf{X} , $\mathbb{P}(\cdot)$ denotes the probability of a random event, and $\|\cdot\|$ denotes the vector 2-norm.

II. PRIOR WORK

In typical communication receiver design, interference is usually modeled as a random variable with Gaussian density distribution [12]. While the Gaussian distribution is a good model for thermal noise at the receiver [13], RFI has predominantly non-Gaussian statistics [14] and is well modeled using impulsive distributions such as symmetric alpha stable [15] and Middleton Class A distributions [16]. The impulsive nature of RFI may cause significant degradation in communication performance of wireless receivers designed under the assumption of additive Gaussian noise [10].

The statistical techniques used in modeling interference can be divided into two categories: (1) statistical inference methods and (2) statistical-physical derivation methods. Statistical inference approaches fit a mathematical model to interference signal measurements, without regard to the physical generation mechanisms behind the interference. Statistical-physical models, on the other hand, model interference based on the physical principles that govern the generation and propagation of interference-causing emissions. Statistical-physical models can therefore be more useful than empirical models in designing robust receivers in the presence of RFI [14]. The following sub-sections discuss key prior results in statistical modeling of RFI in single- and multi-antenna receivers.

A. Prior work in single-antenna RFI models

In [17], it was shown that interference from a homogeneous Poisson field of interferers distributed over the entire plane can be modeled using the symmetric alpha stable distribution [15]. This result was later extended to include channel randomness in [18]. In [14], it was shown that the Middleton Class A distribution well models the statistics of sum interference from a Poisson field of interferers distributed within a circular annular region around the receiver. Their results were generalized in [19], by using the Gaussian mixture distributions to model RFI statistics in network environments with clustered interferers. The Middleton Class A and the Gaussian mixture distributions can also incorporate thermal noise present at the receiver without changing the nature of the distribution, unlike the symmetric alpha stable distribution. The Middleton Class A models are also canonical,

TABLE I: Key statistical models of RFI observed by single-antenna receiver systems

Model Name	Statistical Model	Wireless Network
Symmetric alpha stable	Characteristic Function $\Phi_Y(\omega) = e^{-\sigma \omega ^\alpha}$ α : Characteristic exponent. Range: (0,2] σ : Dispersion parameter. Range: (0,∞)	Decentralized (e.g. <i>ad hoc</i> and femtocells)
Middleton Class A	Amplitude Distribution $f_Y(y) = \sum_{k=0}^{\infty} \frac{e^{-A} A^k}{k! \sqrt{2\pi \frac{k/A+1}{1+\Gamma} \sigma^2}} e^{-\frac{y^2}{2 \frac{k/A+1}{1+\Gamma} \sigma^2}}$ A : Overlap index. Range: (0,∞) Γ : Ratio of Gaussian to non-Gaussian variance. Range: (0,∞) σ^2 : Noise power. Range: (0,∞)	Centralized (e.g. LTE, Wimax, and WiFi)

i.e, no knowledge of the physical environment is needed to estimate the model parameters [20]. The symmetric alpha stable and Middleton Class A distribution functions are listed in Table I.

B. Prior work in multi-antenna RFI models

Prior work on statistical modeling of RFI in multi-antenna wireless systems has typically focused on using multi-variate extensions of single-antenna RFI statistical models, such as the Middleton Class A and symmetric alpha stable distributions. The two common approaches of generating multi-variate extensions of uni-variate distributions assume that either (a) RFI is independent across the receive antennas, or (b) the multi-variate RFI model is isotropic.

In [18], the authors demonstrate the applicability of the spherically isotropic symmetric alpha stable model [21] to RFI generated from a Poisson distributed field of interferers. The authors assume that each receiver is surrounded by the same set of active interferers, and receiver separation is ignored. The spherically isotropic alpha stable model is derived under both homogeneous and non-homogeneous distribution of interferers, with the signal propagation model incorporating pathloss, lognormal shadowing and Rayleigh fading. The study is limited to baseband signaling and neglects any correlation in the interferer to receive antenna channel model or correlation in the interference signal generation model.

In [22], the author proposes three possible extensions to the univariate Class A model. The three multi-dimensional extensions, whose distribution functions are listed in Table II, are as follows:

- 1) MCA.I - Each receive antenna experiences additive uni-variate Class A noise with the identical

parameters. RFI is spatially and temporally independent and identically distributed. MCA.I cannot capture spatial dependence or sample correlation of RFI across receive antennas.

- 2) MCA.II - RFI is assumed to be spatially dependent and correlated across receive antennas. MCA.II can represent correlated or uncorrelated random variables; however, it cannot represent independent Class-A random variables.
- 3) MCA.III - This model incorporates spatial dependence in multi-antenna RFI, but does not support spatial correlation across antenna samples. MCA.III can represent uncorrelated and spatially dependent Class A random variables but it cannot represent independent or correlated random variables.

These models are multi-variate extensions of the Class A distribution and are not derived from physical mechanisms that govern RFI generation. While these models have been very useful in analyzing MIMO receiver performance [23] and designing receiver algorithms [24], a statistical-physical basis for these models would further enhance their appeal [25] in linking wireless network performance with environmental factors such as interferer density, fading parameters, etc.

In [25], the authors attempt to derive RFI statistics for a two antenna receiver based on the statistical-physical mechanisms that produce the RFI. The authors use a physical generation model for the received RFI at each of the two antennas that is the sum of RFI from stochastically placed interferers which include interferers observed by both antennas as well as interferers observed exclusively by a single antenna. Their resulting model is canonical in form, incorporates an additive Gaussian background noise component and has found application in receiver design in the presence of interference [24], [26]. However, it is incomplete as it is strictly limited to two antenna receivers [25], and it enforces statistical dependence among receive antennas similar to MCA.III. This is contrary to their statistical-physical generation mechanism which assumes that each receive antenna has a subset of surrounding interferers that are observed exclusively by that antenna alone. Our article extends their work by using a similar interference generation and propagation framework to develop statistical-physical interference distributions for any number of receive antenna. Table II lists the different joint statistical models of RFI that have been proposed in prior work.

III. SYSTEM MODEL

Consider a wireless communication receiver with N antennas, located in the presence of nearby interfering sources within a two-dimensional plane as shown in Figure 1. The geometry of the individual antenna elements and the inter-antenna spacing is ignored, i.e., the entire receiver is

TABLE II: Key statistical models of RFI observed by multi-antenna receiver systems

Model Name	Statistical Model
Isotropic symmetric alpha stable	Characteristic Function: $\Phi_{\mathbf{Y}}(\mathbf{w}) = e^{-\sigma \ \mathbf{w}\ ^\alpha}$ α : Characteristic exponent σ : Dispersion parameter
Multidimensional Class A – (MCA.I)	Amplitude Distribution: $f_{\mathbf{Y}}(\mathbf{y}) = \prod_{n=1}^N \sum_{k=0}^{\infty} \frac{e^{-A_n} A_n^k}{k! \sqrt{2\pi \frac{k/A_n + \Gamma_n}{1 + \Gamma_n} \sigma_n^2}} e^{-\frac{y_n^2}{2 \frac{k/A_n + \Gamma_n}{1 + \Gamma_n} \sigma_n^2}}$ For each antenna n , A_n : Overlap index Γ_n : Ratio of Gaussian to non-Gaussian noise power σ_n^2 : Noise power
Multidimensional Class A – (MCA.II)	Amplitude Distribution: $f_{\mathbf{Y}}(\mathbf{y}) = \sum_{k=0}^{\infty} \frac{e^{-A} A^k}{k!} \frac{1}{\sqrt{2\pi \frac{k/A + \Gamma}{1 + \Gamma} \Sigma }} e^{-\frac{\mathbf{y}^T \Sigma^{-1} \mathbf{y}}{2 \frac{k/A + \Gamma}{1 + \Gamma}}}$ A : Overlap index Γ : Ratio of Gaussian to non-Gaussian variance Σ : Noise covariance matrix
Multidimensional Class A – (MCA.III)	Amplitude Distribution: $f_{\mathbf{Y}}(\mathbf{y}) = \sum_{k=0}^{\infty} \frac{e^{-A} A^k}{k!} \frac{1}{\sqrt{2\pi \Sigma_k }} e^{-\frac{\mathbf{y}^T \Sigma_k^{-1} \mathbf{y}}{2}}$ $\Sigma_k = (\mathbf{I} + \Gamma)^{-1} \left(\frac{k}{A} \mathbf{I} + \Gamma \right)$ A : Overlap index Γ : Diagonal matrix of Gaussian to non-Gaussian variance ratios
Bivariate Class A	Amplitude Distribution: $f_{\mathbf{n}}(n_1, n_2) = \frac{e^{-A}}{2\pi \mathbf{K}_0 ^{\frac{1}{2}}} e^{-\frac{\mathbf{n}^T \mathbf{K}_0^{-1} \mathbf{n}}{2}} + \frac{(1 - e^{-A})}{2\pi \mathbf{K}_1 ^{\frac{1}{2}}} e^{-\frac{\mathbf{n}^T \mathbf{K}_1^{-1} \mathbf{n}}{2}}$ $\mathbf{K}_m = \begin{bmatrix} \hat{c}_m^2 & \kappa c_m \hat{c}_m \\ \kappa c_m \hat{c}_m & \hat{c}_m^2 \end{bmatrix}, c_m^2 = \frac{m + \Gamma_1}{1 + \Gamma_1}, \hat{c}_m^2 = \frac{m + \Gamma_2}{1 + \Gamma_2}$ A : Overlap index Γ_n : Ratio of Gaussian to non-Gaussian variance at antenna n κ : Correlation coefficient

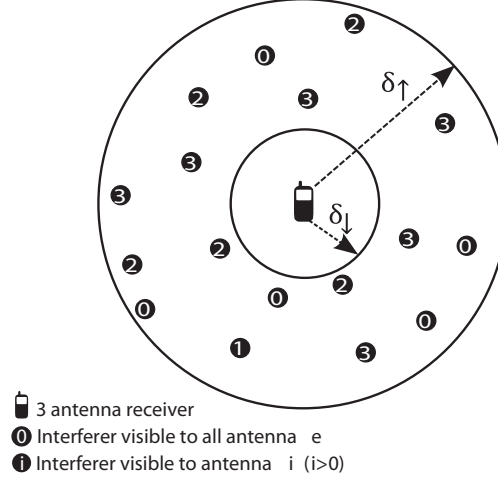


Fig. 1: Illustration of interferer placement around a 3-antenna receiver at a sampling time instant.

assumed to be located at a single point in space. For ease of notation, the origin is shifted to coincide with the receiver location. The interferers are co-planar to the receiver and are transmitting in the same frequency band as the receiver; hence, we can apply the term co-channel interference to describe the resulting RFI. We also assume a fast fading wireless channel and power-law pathloss between the interferers and the receiver.

At each time snapshot, the active interfering sources are classified into $N + 1$ independent sets $\mathcal{S}_0, \mathcal{S}_1, \dots, \mathcal{S}_N$. \mathcal{S}_0 denotes the set of interferers that are observed by all antennas, or in other words, cause interference to every receive antenna. $\mathcal{S}_n \forall n = 1, \dots, N$ denotes the set of interferers that are observed by antenna n alone. At each sampling time instant, we assume that the locations of the active interferers in $\mathcal{S}_n \forall n = 0, \dots, N$ are distributed according to a homogeneous spatial point process with the intensity of set intensity of \mathcal{S}_n denoted by $\lambda_n \forall n = 0, \dots, N$. Based on the intensity of individual interferer fields, our system model yields the following three RFI generation scenarios:

- *Case I* - Interferer set \mathcal{S}_0 is empty, i.e., $\lambda_n > 0$ and $\lambda_0 = 0$. In this scenario, each receiver is under the influence of an independent set of interferers. It is trivial to see that the resulting RFI would also exhibit independence across the receive antennas, i.e., Case I results in RFI that has characteristics of model MCA.I in Table II.
- *Case II* - Interferer sets $\mathcal{S}_n \forall n = 1, \dots, N$ are empty sets, i.e., $\lambda_n = 0$ and $\lambda_0 > 0$. Both receivers observe the same set of interferers, thereby causing the resulting RFI to have spatial dependence across receive antennas. MCA.II and MCA.III from [22], shown in Table II, have the same characteristic in spatial statistics but there is no statistical physical derivation linking these

models to any interference generation mechanism, such as one described in our system model.

- *Case III* - All interferer sets are non-empty, i.e., $\lambda_n > 0$ and $\lambda_0 > 0$. This models partial correlation in the interferer field observed by each of the receive antennas. The common set of interferers in \mathcal{S}_0 models correlation between the interferer fields of two antennas. The level of correlation can be tuned by changing the intensity of the Poisson point process representing each set in the interferer field. This model is quite commonly used in multi-dimensional temporal [27] and spatial interference modeling [25]. The resulting RFI is spatially dependent across receive antennas and neither of MCA.I, MCA.II, or MCA.III appropriately capture the joint spatial statistics of RFI generated in such an environment.

A scenario in which an environment with interferers observed by a subset of receive antennae may arise, is during deployment of receivers employing sectorized antennas with full frequency reuse. Sectorized antennas are geographically co-located wireless directional antennas with radiation patterns shaped as partially overlapping sectors that combine to cover the entire space around the multi-antenna system [28]. Sectorized antennas can provide the advantages of spatial diversity while mitigating the impairments caused by multipath delay [29]. Interference signals common to some antennas may arise in the overlapping sections, i.e., where the antenna gain for all antennas is similar, and individual antennas may still see independent interference in sectors where one antenna exhibits high gain while others exhibit a null.

The Poisson point process is typically used in modeling interferer locations in large wireless networks and provides analytical tractability in mathematical derivations [30]. We wish to highlight the fact that a spatial Poisson point process distribution of interferers allows each interferer set \mathcal{S}_n to have potentially infinite number of interferers. The distance of each interferer from origin (where the receiver is located) provides an ordering function, enabling us to count the interferers in each set. For the i^{th} interfering source in \mathcal{S}_n , $\mathbf{R}_{n,i}$ denotes the two-dimensional coordinates of the interferer's location. Thus, $\|\mathbf{R}_{n,1}\| < \|\mathbf{R}_{n,2}\| < \dots$ is implicitly assumed in order to define the i^{th} interferer at $\mathbf{R}_{n,i}$.

We also assume that the interferers are distributed within a two-dimensional annulus with inner and outer radii δ_{\downarrow} and δ_{\uparrow} , respectively. Based on values of δ_{\downarrow} , our system model supports the following scenarios of interferer placement:

- 1) *Interferer placement with guard-zones*: By allowing $\delta_{\downarrow} > 0$, we constrain the active interferers to be located outside of a finite disk around the multi-antenna wireless receiver, effectively modeling a wireless network with an interferer-free guard zone around the receiver. Such a

TABLE III: Prior results on statistical-physical interference distribution models in multi-antenna receivers. Spatially independent interference is trivially derived from prior work on single-dimensional statistical models of interference. (SAS: Symmetric alpha stable)

Parameter values describing region containing interferers	Spatial dependence		
	Independent (Case I)	Isotropic (Case II)	Continuum (Case III)
$\delta_{\perp} = 0, \delta_{\uparrow} \rightarrow \infty$	Yes [15] (SAS)	Yes [18] (SAS)	No
$\delta_{\perp} = 0, \delta_{\uparrow} < \infty$	No	No	No
$\delta_{\perp} > 0, \delta_{\uparrow} \rightarrow \infty$	Yes [19] (Class A)	No	No
$\delta_{\perp} > 0, \delta_{\uparrow} < \infty$	Yes [19] (Class A)	No	No

model can be applied to cellular and *ad hoc* networks with contention-based or scheduling-based MAC protocols [3]. The joint spatial statistics of the resultant RFI from this model are derived in Section IV-A.

- 2) *Interferer placement without guard-zones*: By setting $\delta_{\perp} = 0$, we allow interferers to be located arbitrarily close to the wireless receiver. Such a scenario can model interference in an *ad hoc* network without any contention-based medium access control protocol [3], as well as platform noise [10] in small form-factor devices such as laptops and mobile phones. The joint spatial statistics of the resultant RFI from this model are derived in Section IV-B.

The possible parameter values $\delta_{\perp} = 0$, $\delta_{\perp} > 0$, $\delta_{\uparrow} < \infty$ and $\delta_{\uparrow} \rightarrow \infty$, combined with the three cases of correlation within interferer distribution, yields a total of twelve possible scenarios of interferer distribution. Table III lists the scenarios where prior statistical models of interference exist in literature. Interference statistics for Case III require knowledge of interference statistics for Cases I and II. The majority of Section IV is dedicated to deriving interference statistics for isotropic interference (Case II) in network scenarios not studied in prior work. The spatially independent interference statistics (Case I) are a trivial extension to the single antenna interference statistics.

IV. JOINT CHARACTERISTIC FUNCTION OF MULTI-ANTENNA RFI

At each receive antenna n , the baseband sum interference signal at any sampling time instant can be expressed as the sum total of the interference signal observed from common interferers and the interference signal from interferers visible only to antenna n . We can express the interference signal at the n^{th} antenna as

$$Y_n = Z_n^0 + Z_n \quad (1)$$

where Z_n, Z_n^0 represent the sum interference signal from interfering sources in \mathcal{S}_n (visible only to antenna n), and interfering sources in \mathcal{S}_0 (visible to all antennas), respectively. The sum interference signal Z_n from interferers in \mathcal{S}_n can be written as [16]

$$Z_n = \sum_{i \in \mathcal{S}_n} B_i^n e^{j\chi_i^n} (D_{n,i})^{-\frac{\gamma}{2}} H_i^n e^{j\Theta_i^n}. \quad (2)$$

Z_n is the sum of interfering signals $B_i^n e^{j\chi_i^n} (D_{n,i})^{-\frac{\gamma}{2}} H_i^n e^{j\Theta_i^n}$ emitted by each interferer $i \in \mathcal{S}_n$ located at $\mathbf{R}_{n,i}$. $B_i^n e^{j\chi_i^n}$ denotes complex baseband emissions from interfering source i where B_i^n is the emission signal envelope and χ_i^n is the phase of the emission. $D_{n,i} = \|\mathbf{R}_{n,i}\|$ denotes the distance between the receiver n (located at origin) and the interferer, and γ is the power pathloss coefficient ($\gamma > 2$), consequently, $(D_{n,i})^{-\frac{\gamma}{2}}$ indicates the reduction in interfering signal amplitude during propagation through the wireless medium. $H_i^n e^{j\Theta_i^n}$ denotes the complex fast-fading channel between the interferer and receiver n . For the fast fading channel model, we assume that the channel amplitude H_i^n follows the Rayleigh distribution, and that the channel phase Θ_i^n is uniformly distributed on $[0, 2\pi]$. H_i^n, Θ_i^n, B_i^n , and χ_i^n are assumed to be *i.i.d.* across all interfering sources $i \in \mathcal{S}_n$. In Sections V-A to V-D, we study the impact of removing many of these assumptions on the statistics of RFI.

The signal from the common set of interferers \mathcal{S}_0 is expressed as

$$Z_n^0 = \sum_{i^0 \in \mathcal{S}_0} B_i^0 e^{j\chi_i^0} (D_{0,i})^{-\frac{\gamma}{2}} H_{n,i}^0 e^{j\Theta_{n,i}^0}. \quad (3)$$

Note that the difference between (2) and (3) is that the interferer emission signal $B_i^0 e^{j\chi_i^0}$ and the distance $D_{0,i}$ between interferer i and the receive antenna n (placed at origin), is independent of the antenna under observation (n). This is because we ignore inter-antenna spacing and assume all antennas are located at the origin. The channel between the interferer and n^{th} receiver, denoted by $H_{n,i}^0 e^{j\Theta_{n,i}^0}$, is also assumed *i.i.d.* across n and i . In Section V-C, we will discuss the impact of spatial correlation of the channel model on interference statistics. Combining (1), (2), and (3) we can write the resultant interference signal at the n^{th} receive antenna as

$$Y_n = \sum_{i_0 \in \mathcal{S}_0} B_{i_0}^0 D_{0,i_0}^{-\frac{\gamma}{2}} H_{n,i_0}^0 e^{j(\chi_{i_0}^0 + \Theta_{n,i_0}^0)} + \sum_{i \in \mathcal{S}_n} B_i^n D_{n,i}^{-\frac{\gamma}{2}} H_i^n e^{j(\chi_i^n + \Theta_i^n)}. \quad (4)$$

The complex baseband interference at each receive antenna can then be decomposed into its in-phase and quadrature components $Y_n = Y_{n,I} + jY_{n,Q}$, where

$$Y_{n,I} = \sum_{i_0 \in \mathcal{S}_0} B_{i_0}^0 D_{0,i_0}^{-\frac{\gamma}{2}} H_{n,i_0}^0 \cos(\chi_{i_0}^0 + \Theta_{n,i_0}^0) + \sum_{i \in \mathcal{S}_n} B_i^n D_{n,i}^{-\frac{\gamma}{2}} H_i^n \cos(\chi_i^n + \Theta_i^n), \quad (5)$$

and

$$Y_{n,Q} = \sum_{i_0 \in \mathcal{S}_0} B_{i_0}^0 D_{0,i_0}^{-\frac{\gamma}{2}} H_{n,i_0}^0 \sin(\chi_{i_0}^0 + \Theta_{n,i_0}^0) + \sum_{i \in \mathcal{S}_n} B_i^n D_{n,i}^{-\frac{\gamma}{2}} H_i^n \sin(\chi_i^n + \Theta_i^n). \quad (6)$$

In order to study the spatial statistics of interference across multiple receive antennas, we will derive the joint characteristic function of the in-phase and quadrature-phase components of interference. Using (1), (5) and (6), the joint characteristic function $\Phi_{\mathbf{Y}}$ can be written as

$$\Phi_{\mathbf{Y}}(\mathbf{w}) = \mathbb{E} \left\{ e^{\sum_{n=1}^N j\omega_{n,I} Y_{n,I} + j\omega_{n,Q} Y_{n,Q}} \right\} \quad (7)$$

where $\mathbf{w} = [\omega_{1,I} \ \omega_{1,Q} \ \omega_{2,I} \ \omega_{2,Q} \ \cdots \ \omega_{N,I} \ \omega_{N,Q}]$. Note that the expectation is evaluated over the random variables $|\mathcal{S}_0|$, $|\mathcal{S}_n|$, $D_{0,i}$, $D_{n,i}$, $H_{n,i}^0$, H_i^n , B_i^0 , B_i^n , χ_i^0 , χ_i^n , $\Theta_{n,i}^0$ and $\Theta_i^n \ \forall n = 1, \dots, N$. For the sake of brevity and readability, we refrain from listing all of these random variables in the subscript of the expectation operator. We can separate the independent terms in the expectation by noting that the interferers in the different sets \mathcal{S}_n are distributed in space as independent homogeneous processes, and their emissions and channel realizations are also independent as well. Substituting (4) in (7) and separating independent terms in the expectation, we get

$$\begin{aligned} \Phi_{\mathbf{Y}}(\mathbf{w}) &= \prod_{n=1}^N \mathbb{E} \left\{ e^{j \sum_{i=1}^{|\mathcal{S}_n|} D_{n,i}^{-\frac{\gamma}{2}} H_i^n B_i^n (\omega_{n,I} \cos(\chi_i^n + \Theta_i^n) + \omega_{n,Q} \sin(\chi_i^n + \Theta_i^n))} \right\} \\ &\quad \times \mathbb{E} \left\{ e^{j \sum_{n=1}^N \sum_{i_0=1}^{|\mathcal{S}_0|} D_{0,i_0}^{-\frac{\gamma}{2}} H_{n,i_0}^0 B_{i_0}^0 (\omega_{n,I} \cos(\chi_{i_0}^0 + \Theta_{n,i_0}^0) + \omega_{n,Q} \sin(\chi_{i_0}^0 + \Theta_{n,i_0}^0))} \right\}. \end{aligned} \quad (8)$$

To simplify notation, (8) is decomposed into the product form

$$\Phi_{\mathbf{Y}}(\mathbf{w}) = \Phi_{\mathbf{Y},\mathcal{S}_0}(\mathbf{w}) \prod_{n=1}^N \Phi_{\mathbf{Y},\mathcal{S}_n}(\mathbf{w}) \quad (9)$$

where,

$$\Phi_{\mathbf{Y},\mathcal{S}_0}(\mathbf{w}) = \mathbb{E} \left\{ e^{j \sum_{n=1}^N \sum_{i_0=1}^{|\mathcal{S}_0|} D_{0,i_0}^{-\frac{\gamma}{2}} H_{n,i_0}^0 B_{i_0}^0 (\omega_{n,I} \cos(\chi_{i_0}^0 + \Theta_{n,i_0}^0) + \omega_{n,Q} \sin(\chi_{i_0}^0 + \Theta_{n,i_0}^0))} \right\} \quad (10)$$

$$\Phi_{\mathbf{Y},\mathcal{S}_n}(\mathbf{w}) = \mathbb{E} \left\{ e^{j \sum_{i=1}^{|\mathcal{S}_n|} D_{n,i}^{-\frac{\gamma}{2}} H_i^n B_i^n (\omega_{n,I} \cos(\chi_i^n + \Theta_i^n) + \omega_{n,Q} \sin(\chi_i^n + \Theta_i^n))} \right\}. \quad (11)$$

Each component term in (9) is the characteristic function of the interference contribution by one of each interferer sets $\{\mathcal{S}_0, \mathcal{S}_1, \dots, \mathcal{S}_N\}$. We can rewrite (10) and (11) in their polar forms as

$$\Phi_{\mathbf{Y},\mathcal{S}_0}(\mathbf{w}) = \mathbb{E} \left\{ e^{j \sum_{n=1}^N |\bar{\omega}_n| \sum_{i=1}^{|\mathcal{S}_0|} D_{0,i}^{-\frac{\gamma}{2}} H_{n,i}^0 B_i^0 \cos(\chi_i^0 + \Theta_{n,i}^0 + \xi_{\omega,n})} \right\} \quad (12)$$

$$\Phi_{\mathbf{Y},\mathcal{S}_n}(\mathbf{w}) = \mathbb{E} \left\{ e^{j |\bar{\omega}_n| \sum_{i=1}^{|\mathcal{S}_n|} D_{n,i}^{-\frac{\gamma}{2}} H_i^n B_i^n \cos(\chi_i^n + \Theta_i^n + \xi_{\omega,n})} \right\} \quad (13)$$

where $|\bar{\omega}_n| = \sqrt{\omega_{n,I}^2 + \omega_{n,Q}^2}$ and $\xi_{\omega,n} = \tan^{-1} \left(\frac{\omega_{n,I}}{\omega_{n,Q}} \right)$. We will now evaluate each component term in (9) for interferer environments with and without guard zones, as described in Section III.

A. Joint spatial statistics of RFI in presence of guard zones

1) *Evaluation of $\Phi_{\mathbf{Y}, \mathcal{S}_0}(\mathbf{w})$ (RFI contribution from \mathcal{S}_0):* In this section, we evaluate the contribution of the interferers in set \mathcal{S}_0 to the joint spatial statistics of RFI, denoted by the term $\Phi_{\mathbf{Y}, \mathcal{S}_0}(\mathbf{w})$ in (7). In the constrained interferer placement system model, the interferers within \mathcal{S}_0 are distributed according to a homogeneous spatial Poisson point process inside an annulus with finite inner and outer radii δ_{\downarrow} and δ_{\uparrow} , respectively. Consequently, the number of interferers $|\mathcal{S}_0|$ is a Poisson random variable with parameter $\lambda\pi(\delta_{\uparrow}^2 - \delta_{\downarrow}^2)$. Conditioned on $|\mathcal{S}_0|$, (12) can be expressed as

$$\Phi_{\mathbf{Y}, \mathcal{S}_0}(\mathbf{w}) = \mathbb{E} \left\{ e^{j \sum_{n=1}^N |\bar{\omega}_n| \sum_{i=1}^{|\mathcal{S}_0|} D_{0,i}^{-\frac{\gamma}{2}} H_{n,i}^0 B_i^0 \cos(\chi_i^0 + \Theta_{n,i}^0 + \xi_{\omega,n})} \right\} \quad (14)$$

$$= \sum_{k=0}^{\infty} \mathbb{E} \left\{ e^{j \sum_{n=1}^N |\bar{\omega}_n| \sum_{i=1}^k D_{0,i}^{-\frac{\gamma}{2}} H_{n,i}^0 B_i^0 \cos(\chi_i^0 + \Theta_{n,i}^0 + \xi_{\omega,n})} \middle| |\mathcal{S}_0| = k \right\} \mathbb{P}(|\mathcal{S}_0| = k) \quad (15)$$

$$= \sum_{k=0}^{\infty} \mathbb{E} \left\{ e^{j \sum_{n=1}^N |\bar{\omega}_n| D_0^{-\frac{\gamma}{2}} H_n^0 B^0 \cos(\chi^0 + \Theta_n^0 + \xi_{\omega,n})} \right\}^k \mathbb{P}(|\mathcal{S}_0| = k) \quad (16)$$

Once conditioned on a fixed number of total points, the points in a Poisson point process are distributed independently and uniformly across the region in consideration. This allows us to remove the interferer index i and treat the contribution to RFI from each interferer as an independent random variable. $H_{n,i}^0$, $B_{n,i}^0$, $\chi_{n,i}^0$ and $\Theta_{n,i}^0$ are all *i.i.d.* and can be replaced in (16) by H_n^0 , B_n^0 , χ_n^0 and Θ_n^0 , respectively. $D_{0,i}$ is assumed to be increasing with the index i , since we assumed that the interferers are ordered according to how close they are located to the origin. However, by virtue of a property of Poisson point processes, the points are uniformly distributed within the region of the point process when conditioned on the total number of points k . Thus, in (16) we replaced $D_{0,i}$ by the random variable D_0 , that follows the distribution

$$f_{D_0|k}(D_0|k) = \begin{cases} \frac{2D_0}{\delta_{\uparrow}^2 - \delta_{\downarrow}^2} & \text{if } \delta_{\downarrow} \leq D_0 \leq \delta_{\uparrow}, \\ 0 & \text{otherwise.} \end{cases}$$

This distribution arises when we consider the annular disc with inner and outer radius of δ_{\downarrow} and δ_{\uparrow} , and k points distributed uniformly in this region. The number of interferers (k) within the annular region is a Poisson random variable with mean $\lambda_0\pi(\delta_{\uparrow}^2 - \delta_{\downarrow}^2)$. Combining this notion with (16) we get

$$\Phi_{\mathbf{Y}, \mathcal{S}_0}(\mathbf{w}) = \sum_{k=0}^{\infty} \mathbb{E} \left\{ e^{j \sum_{n=1}^N |\bar{\omega}_n| D_0^{-\frac{\gamma}{2}} H_n^0 B^0 \cos(\chi^0 + \Theta_n^0 + \xi_{\omega,n})} \right\}^k e^{-\lambda_0\pi(\delta_{\uparrow}^2 - \delta_{\downarrow}^2)} \frac{(\lambda_0\pi(\delta_{\uparrow}^2 - \delta_{\downarrow}^2))^k}{k!} \quad (17)$$

$$= e^{-\lambda_0\pi(\delta_{\uparrow}^2 - \delta_{\downarrow}^2)} \sum_{k=0}^{\infty} \frac{\left[(\lambda_0\pi(\delta_{\uparrow}^2 - \delta_{\downarrow}^2)) \mathbb{E} \left\{ e^{j \sum_{n=1}^N |\bar{\omega}_n| D_0^{-\frac{\gamma}{2}} H_n^0 B^0 \cos(\chi^0 + \Theta_n^0 + \xi_{\omega,n})} \right\} \right]^k}{k!} \quad (18)$$

$$= e^{-\lambda_0 \pi (\delta_1^2 - \delta_1^2)} e^{\mathbb{E} \left\{ e^{j \sum_{n=1}^N |\bar{\omega}_n| D_0^{-\frac{\gamma}{2}} H_n^0 B^0 \cos(\chi^0 + \Theta_n^0 + \xi_{\omega, n})} \right\} \lambda_0 \pi (\delta_1^2 - \delta_1^2)} \quad (19)$$

$$= e^{\left[\mathbb{E} \left\{ e^{j \sum_{n=1}^N |\bar{\omega}_n| D_0^{-\frac{\gamma}{2}} H_n^0 B^0 \cos(\chi^0 + \Theta_n^0 + \xi_{\omega, n})} \right\} - 1 \right] \lambda_0 \pi (\delta_1^2 - \delta_1^2)} \quad (20)$$

By taking the logarithm of $\Phi_{\mathbf{Y}, \mathcal{S}_0}(\mathbf{w})$ in (20), the log-characteristic function is

$$\Psi_{\mathbf{Y}, \mathcal{S}_0}(\mathbf{w}) \triangleq \log \Phi_{\mathbf{Y}, \mathcal{S}_0}(\mathbf{w}) \quad (21)$$

$$= \lambda_0 \pi (\delta_1^2 - \delta_1^2) \left(\mathbb{E} \left\{ e^{j \sum_{n=1}^N |\bar{\omega}_n| D_0^{-\frac{\gamma}{2}} H_n^0 B^0 \cos(\chi^0 + \Theta_n^0 + \xi_{\omega, n})} \right\} - 1 \right) \quad (22)$$

$$= \bar{K} \left(\mathbb{E} \left\{ \prod_{n=1}^N e^{j |\bar{\omega}_n| D_0^{-\frac{\gamma}{2}} H_n^0 B^0 \cos(\chi^0 + \Theta_n^0 + \xi_{\omega, n})} \right\} - 1 \right) \quad (23)$$

where $\bar{K} = \lambda_0 \pi (\delta_1^2 - \delta_1^2)$. Next we use the identity

$$e^{j a \cos(b)} = \sum_{m=0}^{\infty} j^m \epsilon_m J_m(a) \cos(mb) \quad (24)$$

where $\epsilon_0 = 1$, $\epsilon_m = 2$ for $m \geq 1$, and $J_m(\cdot)$ denotes the Bessel function of order m . Combining (24) and (23), the log-characteristic function $\Psi_{\mathbf{Y}, \mathcal{S}_0}(\mathbf{w})$ can be expressed as

$$\Psi_{\mathbf{Y}, \mathcal{S}_0}(\mathbf{w}) = \bar{K} \left(\mathbb{E} \left\{ \prod_{n=1}^N \sum_{m_n=0}^{\infty} j^{m_n} \epsilon_{m_n} J_{m_n} \left(|\bar{\omega}_n| D_0^{-\frac{\gamma}{2}} H_n^0 B^0 \cos(m_n (\chi^0 + \Theta_n^0 + \xi_{\omega, n})) \right) \right\} - 1 \right). \quad (25)$$

Since χ^0 and Θ_n^0 are uniform random variables within $[0, 2\pi]$, for any value of $\xi_{\omega, n}$ and m_n , $m_n (\chi^0 + \Theta_n^0 + \xi_{\omega, n})$ modulo 2π is also uniformly distributed over $[0, 2\pi]$. Thus, all terms in (25) with $m_n > 0 \forall n = 1 \rightarrow N$ reduce to zero after taking expectation with respect to Θ_n^0 , and (25) reduces to

$$\Psi_{\mathbf{Y}, \mathcal{S}_0}(\mathbf{w}) = \bar{K} \left(\mathbb{E} \left\{ \prod_{n=1}^N J_0 \left(|\bar{\omega}_n| D_0^{-\frac{\gamma}{2}} H_n^0 B^0 \right) \right\} - 1 \right). \quad (26)$$

Note that the expectation is now with respect to the remaining random variables in (26). To evaluate the expectation in (26), we rewrite it as

$$\Psi_{\mathbf{Y}, \mathcal{S}_0}(\mathbf{w}) = \bar{K} \left(\mathbb{E} \left\{ \prod_{n=1}^N \mathbb{E}_{H_n^0} \left\{ J_0 \left(|\bar{\omega}_n| D_0^{-\frac{\gamma}{2}} H_n^0 B^0 \right) \right\} \right\} - 1 \right). \quad (27)$$

Note that we used the assumption that the fast-fading channel between interferer and receive antennas are spatially independent across the antenna index n . Using the series expansion of the zero-th order Bessel function,

$$J_0(x) = \sum_{m=0}^{\infty} \frac{(-1)^m x^{2m}}{2^{2m} m! \Gamma(m+1)} \quad (28)$$

we can rewrite (27) as

$$\Psi_{\mathbf{Y}, \mathcal{S}_0}(\mathbf{w}) = \bar{K} \left(\mathbb{E} \left\{ \prod_{n=1}^N \mathbb{E}_{H_n^0} \left\{ \sum_{m=0}^{\infty} \frac{(-1)^m \left(|\bar{\omega}_n| D_0^{-\frac{\gamma}{2}} H_n^0 B^0 \right)^{2m}}{2^{2m} m! \Gamma(m+1)} \right\} \right\} - 1 \right) \quad (29)$$

$$= \bar{K} \left(\mathbb{E} \left\{ \prod_{n=1}^N \sum_{m=0}^{\infty} \frac{(-1)^m \left(|\bar{\omega}_n| D_0^{-\frac{\gamma}{2}} B^0 \right)^{2m} \mathbb{E}_{H_n^0} \{ (H_n^0)^{2m} \}}{2^{2m} m! \Gamma(m+1)} \right\} - 1 \right) \quad (30)$$

Under the assumption that the fading channel is Rayleigh distributed, the $2m^{\text{th}}$ moment of H_n^0 is $(\mathbb{E}\{H^{0^2}\})^m \Gamma(1+m)$. Applying to (30), we get

$$\Psi_{\mathbf{Y}, \mathcal{S}_0}(\mathbf{w}) = \bar{K} \left(\mathbb{E} \left\{ \prod_{n=1}^N \sum_{m=0}^{\infty} \frac{(-1)^m \left(|\bar{\omega}_n| D_0^{-\frac{\gamma}{2}} B^0 \right)^{2m} (\mathbb{E}\{H^{0^2}\})^m \Gamma(1+m)}{2^{2m} m! \Gamma(m+1)} \right\} - 1 \right) \quad (31)$$

$$= \bar{K} \left(\mathbb{E} \left\{ \prod_{n=1}^N \sum_{m=0}^{\infty} \frac{(-1)^m \left(|\bar{\omega}_n| D_0^{-\frac{\gamma}{2}} B^0 \sqrt{\mathbb{E}\{H^{0^2}\}} \right)^{2m}}{2^{2m} m!} \right\} - 1 \right) \quad (32)$$

$$= \bar{K} \left(\mathbb{E} \left\{ \prod_{n=1}^N e^{-\frac{\left(|\bar{\omega}_n| D_0^{-\frac{\gamma}{2}} B^0 \sqrt{\mathbb{E}\{H^{0^2}\}} \right)^2}{4}} \right\} - 1 \right) \quad (33)$$

$$= \bar{K} \left(\mathbb{E} \left\{ e^{-\frac{\left(D_0^{-\frac{\gamma}{2}} B^0 \right)^2 \mathbb{E}\{H^{0^2}\} \|\mathbf{w}\|^2}{4}} \right\} - 1 \right). \quad (34)$$

Expanding the expectation in (34) with respect to the random variable D_0 , we have

$$\Psi_{\mathbf{Y}, \mathcal{S}_0}(\mathbf{w}) = \lim_{\delta_{\uparrow} \rightarrow \infty} \bar{K} \left(\mathbb{E} \left\{ \int_{\delta_{\downarrow}}^{\delta_{\uparrow}} e^{-\|\mathbf{w}\|^2 \left(D_0^{-\frac{\gamma}{2}} B^0 \right)^2 \mathbb{E}\{H^{0^2}\}} \frac{2D_0}{\delta_{\uparrow}^2 - \delta_{\downarrow}^2} dD_0 \right\} - 1 \right) \quad (35)$$

Using Taylor series expansion of e^x , (35) can be written as

$$\Psi_{\mathbf{Y}, \mathcal{S}_0}(\mathbf{w}) = \lim_{\delta_{\uparrow} \rightarrow \infty} \bar{K} \left(\mathbb{E} \left\{ \int_{\delta_{\downarrow}}^{\delta_{\uparrow}} \sum_{m=1}^{\infty} \frac{(-1)^m D_0^{-\frac{m\gamma}{2}} \mathbb{E}\{(B^0)^{2m}\} (\mathbb{E}\{H^{0^2}\})^m \|\mathbf{w}\|^{2m}}{4^m m!} \frac{2D_0}{\delta_{\uparrow}^2 - \delta_{\downarrow}^2} dD_0 \right\} - 1 \right) \quad (36)$$

$$= \lambda_0 \pi \left(\sum_{m=1}^{\infty} \frac{(-1)^m D_0^{-\frac{m\gamma}{2}} \mathbb{E}\{(B^0)^{2m}\} (\mathbb{E}\{H^{0^2}\})^m \|\mathbf{w}\|^{2m} (\delta_{\downarrow}^{-\gamma m - 2} - \delta_{\uparrow}^{-\gamma m - 2})}{4^m m!} \frac{2}{m\gamma - 2} \right) \quad (37)$$

valid for $\gamma > 2$. Assuming that the interferer emission amplitude B^0 has constant value \bar{B} , we get

$$\Psi_{\mathbf{Y}, \mathcal{S}_0}(\mathbf{w}) = \lambda \pi \sum_{m=1}^{\infty} \frac{(-1)^m (\|\mathbf{w}\|^2 \sigma \bar{B})^m \delta_{\downarrow}^{-\gamma m + 2}}{4^m m!} \frac{2}{\gamma m - 2} \left(1 - \frac{\delta_{\uparrow}^{-\gamma m - 2}}{\delta_{\downarrow}} \right) \quad (38)$$

In Section V-A, we discuss the impact of applying any general interferer emission amplitude distribution on the interference statistics. The multiplicative term $\frac{2}{m\gamma - 2} \left(1 - \frac{\delta_{\uparrow}^{-\gamma m - 2}}{\delta_{\downarrow}} \right)$ prevents us from

simplifying (38) into an exponential. Note that in reasonable to assume that for many wireless network scenarios $\delta_\uparrow \gg \delta_\downarrow$, in which case $\left(1 - \frac{\delta_\downarrow}{\delta_\uparrow} \gamma^{m-2}\right) \rightarrow 1$ and we are left with the term $\frac{2}{m\gamma-2}$. Similar to an approach used in [19], we approximate $\frac{2}{m\gamma-2}$ as an power series $\eta\beta^m$ for $m \geq 1$ and choose parameters η_γ and β_γ to minimize the mean squared error (MSE)

$$\{\eta_\gamma, \beta_\gamma\} = \arg \min_{\eta \in \mathbb{R}, \beta \in \mathbb{R}} \sum_{m=1}^{\infty} \left(\frac{2}{m\gamma-2} - \eta\beta^m \right)^2. \quad (39)$$

Using the non-linear unconstrained optimization functionality provided by MATLAB, we are able to determine the appropriate values for $\{\eta_\gamma, \beta_\gamma\}$ for any $\gamma > 2$ with MSE less than 10^{-4} . In the case where $\left(1 - \frac{\delta_\downarrow}{\delta_\uparrow} \gamma^{m-2}\right)$ cannot be ignored, we can again use the power series approximation to find parameters $\{\eta_\gamma, \beta_\gamma\}$ such that $\{\eta_\gamma, \beta_\gamma\} = \arg \min_{\eta \in \mathbb{R}, \beta \in \mathbb{R}} \sum_{m=1}^{\infty} \left(\frac{2}{m\gamma-2} \left(1 - \frac{\delta_\downarrow}{\delta_\uparrow} \gamma^{m-2}\right) - \eta\beta^m \right)^2$.

Using the aforementioned approximation, the log-characteristic exponent in (38) can be expressed as

$$\Psi_{\mathbf{Y}, \mathcal{S}_0}(\mathbf{w}) = \lambda\pi \sum_{m=1}^{\infty} \frac{(-1)^m (\|\mathbf{w}\|^2 \sigma \bar{B})^m \delta_\downarrow^{-\gamma m+2}}{4^m m!} \eta_\gamma \beta_\gamma^m \quad (40)$$

$$= \lambda\pi \delta_\downarrow^2 \eta_\gamma \left(e^{-\frac{\|\mathbf{w}\|^2 \delta_\downarrow^{-\gamma} \beta_\gamma \mathbb{E}\{H^{0^2}\} \bar{B}^2}{4}} - 1 \right) \quad (41)$$

$$= A_0 \left(e^{-\frac{\|\mathbf{w}\|^2 \Omega_0}{2}} - 1 \right). \quad (42)$$

(40) is the log-characteristic function of a Middleton Class A where $A_0 = \lambda\pi \delta_\downarrow^2 \eta_\gamma$ is the overlap index indicating the impulsiveness of the interference, and $\Omega_0 = \frac{A_0 \delta_\downarrow^{-\gamma} \beta_\gamma \mathbb{E}\{H^{0^2}\} \bar{B}^2}{2}$ is the mean intensity of the interference [14]. Thus, we can write (10) as

$$\Phi_{\mathbf{Y}, \mathcal{S}_0}(\mathbf{w}) = e^{A_0 \left(e^{-\frac{\|\mathbf{w}\|^2 \Omega_0}{2}} - 1 \right)} \quad (43)$$

which is the characteristic function of the isotropic multi-variate Middleton Class A distribution shown in Table II as MCA.II or more generally, MCA.III with a Γ containing equal values in the diagonal. The next section incorporates receiver thermal noise which gives rise to the Γ parameter seen in MCA.II and MCA.III.

2) *Evaluation of $\Phi_{\mathbf{Y}, \mathcal{S}_n}(\mathbf{w})$ (RFI contribution from \mathcal{S}_n):* In this section, we derive contribution of interferer sets $\mathcal{S}_i \forall i = 1, 2, \dots, N$ to the spatial joint statistics of RFI. At each antenna n , the interference from the exclusive set of interferers is identical to RFI seen by a single antenna receiver surrounded by interferers distributed according to a Poisson point process. The statistics of such RFI have been derived in [19] and shown to be well modeled by the univariate Middleton Class A distribution. Thus

we can write (11) as

$$\Phi_{\mathbf{Y}, \mathcal{S}_n}(\mathbf{w}) = e^{A_n \left(e^{-\frac{\|\mathbf{w}\|^2 \Omega_n}{2}} - 1 \right)} \quad (44)$$

where $A_n = \lambda_n \pi \delta_{\perp}^2 \eta_{\gamma}$ and $\Omega_n = \frac{A_n \delta_{\perp}^{-\gamma} \mathbb{E}\{H^{n^2}\} \overline{B}^2 \beta_{\gamma}}{2}$ are the parameters of the Class A distribution. Combining (9), (43) and (44), we get the joint characteristic function of RFI as

$$\Phi_{\mathbf{Y}}(\mathbf{w}) = e^{A_0 \left(e^{-\frac{\|\mathbf{w}\|^2 \Omega_0}{2}} - 1 \right)} \times \prod_{n=1}^N e^{A_n \left(e^{-\frac{\|\mathbf{w}\|^2 \Omega_n}{2}} - 1 \right)}. \quad (45)$$

The corresponding probability density function can be written as

$$f(\mathbf{Y}) = \left\{ \prod_{n=1}^N \left\{ \sum_{m_n=1}^{\infty} \frac{e^{-A_n} (A_n)^{m_n}}{\sqrt{2\pi m_n \Omega_n} m_n!} e^{-\frac{\|\mathbf{Y}_n\|^2}{2m_n \Omega_n}} + e^{-A_n} \delta(\mathbf{Y}_n) \right\} \right\} \times \sum_{m_0=1}^{\infty} \frac{e^{-A_0} (A_0)^{m_0}}{\sqrt{2\pi m_0 \Omega_0} m_0!} e^{-\frac{\|\mathbf{Y}\|^2}{2m_0 \Omega_0}} + e^{-A_0} \delta(\mathbf{Y}) \quad (46)$$

where $\delta(\cdot)$ is the Dirac-delta function. It indicates the probability that there are no interferers in the annular region around the receiver, resulting in zero RFI. In practical receivers, however, thermal background noise is always present and is well modeled by the Gaussian distribution. Assuming that antenna n observes independent thermal noise with variance ρ_n , we can incorporate it into our model resulting in the following distribution

$$f(\mathbf{Y}) = \left\{ \prod_{n=1}^N \left\{ \sum_{m_n=0}^{\infty} \frac{e^{-A_n} (A_n)^{m_n}}{\sqrt{2\pi \Omega_n (m_n + \Gamma_n)} m_n!} e^{-\frac{\|\mathbf{Y}_n\|^2}{2\Omega_n (m_n + \Gamma_n)}} \right\} \right\} \sum_{m_0=1}^{\infty} \frac{e^{-A_0} (A_0)^{m_0}}{\sqrt{2\pi m_0 \Omega_0} m_0!} e^{-\frac{\|\mathbf{Y}\|^2}{2m_0 \Omega_0}} + e^{-A_0} \prod_{n=1}^N \sum_{m_n=0}^{\infty} \frac{e^{-A_n} (A_n)^{m_n}}{\sqrt{2\pi m_n \Omega_n} m_n!} e^{-\frac{\|\mathbf{Y}_n\|^2}{2\Omega_n (m_n + \Gamma_n)}} \quad (47)$$

where $\Gamma_n = \frac{\rho_n}{\Omega_n}$.

It is interesting to note that the parameter A_n ($n = 1, \dots, N$) is linearly dependent on the corresponding interferer density λ_n . If λ_n is very high, or in other words, the number of interferers becomes very large, A_n grows large as well and it is well known that for large values of A_n , the Middleton Class A distribution is less impulsive in nature and resembles the Gaussian distribution. Thus, asymptotically increasing the number of interferers changes the nature of the distribution as well. Since A_n is also proportional to δ_{\perp}^2 , we can see that the interference statistics become less impulsive as the radius of the guard zone increases.

B. Joint spatial statistics of RFI in absence of guard-zones

In this section, we derive joint spatial statistics of sum interference with the parameter $\delta_{\perp} = 0$. In the absence of guard zones, an active interferer may arise quite close to the receiver causing a sudden large burst of interference. Such events cause a high degree of impulsiveness in interference subsequently leading to heavy-tails in first-order interference statistics.

1) *Evaluation of $\Phi_{\mathbf{Y},\mathcal{S}_0}(\mathbf{w})$ (RFI contribution from \mathcal{S}_0):* The contribution to the joint spatial statistics of RFI from the interferers in \mathcal{S}_0 is expressed as the term $\Phi_{\mathbf{Y},\mathcal{S}_0}(\mathbf{w})$ in the joint characteristic function of RFI given by (9). In order to derive closed form expressions for (10), we set $\delta_{\downarrow} = 0$ in (35) to get

$$\Psi_{\mathbf{Y},\mathcal{S}_0}(\mathbf{w}) = \lambda_0 \pi \delta_{\uparrow}^2 \left(\mathbb{E} \left\{ \int_0^{\delta_{\uparrow}} \left(e^{-\|\mathbf{w}\|^2 \left(D_0^{-\frac{\gamma}{2}} B^0 \right)^2 \mathbb{E}\{H^{0^2}\}} - 1 \right) \frac{2D_0}{\delta_{\uparrow}^2} dD_0 \right\} \right) \quad (48)$$

Combining $\|\mathbf{w}\|^2$ and $D_0^{-\gamma}$ into a temporary variable $E_0 = D_0 \|\mathbf{w}\|^{\frac{2}{\gamma}}$, we get

$$\Psi_{\mathbf{Y},\mathcal{S}_0}(\mathbf{w}) = \lambda_0 \pi \left(\mathbb{E} \left\{ \|\mathbf{w}\|^{\frac{4}{\gamma}} \int_0^{\delta_{\uparrow} \|\mathbf{w}\|^{\frac{2}{\gamma}}} \left(e^{-\left(E_0^{-\frac{\gamma}{2}} B^0 \right)^2 \mathbb{E}\{H^{0^2}\}} - 1 \right) 2E_0 dE_0 \right\} \right) \quad (49)$$

When $\delta_{\uparrow} \rightarrow \infty$, the integral is reduced to

$$\Psi_{\mathbf{Y},\mathcal{S}_0}(\mathbf{w}) = \lambda_0 \pi \|\mathbf{w}\|^{\frac{4}{\gamma}} \mathbb{E} \left\{ \int_0^{\infty} \left(e^{-\left(E_0^{-\frac{\gamma}{2}} B^0 \right)^2 \mathbb{E}\{H^{0^2}\}} - 1 \right) 2E_0 dE_0 \right\} \quad (50)$$

consequently, the characteristic function $\Phi_{\mathbf{Y},\mathcal{S}_0}(\mathbf{w})$ is of the form

$$\Phi_{\mathbf{Y},\mathcal{S}_0}(\mathbf{w}) = e^{-\sigma_0 \|\mathbf{w}\|^\alpha} \quad (51)$$

where $\alpha = \frac{4}{\gamma}$, and $\sigma_0 = \lambda_0 \pi \mathbb{E} \left\{ \int_0^{\infty} 1 - e^{-\left(E_0^{-\frac{\gamma}{2}} B^0 \right)^2 \mathbb{E}\{H^{0^2}\}} 2E_0 dE_0 \right\}$. This is the characteristic function of an isotropic symmetric alpha stable random vector. The characteristic function expression in (49) offers little insight when δ_{\uparrow} is finite, however, it has been shown in [18] that a series summation of the form (4) with finite terms converges very rapidly to the alpha stable distribution.

2) *Evaluation of $\Phi_{\mathbf{Y},\mathcal{S}_n}(\mathbf{w})$ (RFI contribution from \mathcal{S}_n):* $\Phi_{\mathbf{Y},\mathcal{S}_n}(\mathbf{w})$ can be considered as the contribution to the joint characteristic function of RFI, made by interfering sources visible only to one receive antenna. The evaluation of $\Phi_{\mathbf{Y},\mathcal{S}_n}(\mathbf{w})$ for interferers in \mathcal{S}_n is identical for all $n = 1, 2, \dots, N$. Starting with (13) and Using a derivation similar to the steps from (16) to (25), we get that

$$\log \Phi_{\mathbf{Y},\mathcal{S}_n}(\mathbf{w}) = \lambda_n \pi \delta_{\uparrow}^2 \mathbb{E} \left\{ J_0 \left(|\bar{\omega}_n| D_n^{-\frac{\gamma}{2}} H_n B^0 \right) - 1 \right\} \quad (52)$$

Taking expectation over D_n with our knowledge of the distribution of D_n , we get

$$\log \Phi_{\mathbf{Y},\mathcal{S}_n}(\mathbf{w}) = \lambda_n \pi \delta_{\uparrow}^2 \int_0^{\delta_{\uparrow}} \mathbb{E} \left\{ J_0 \left(|\bar{\omega}_n| D_n^{-\frac{\gamma}{2}} H_n B^0 \right) - 1 \right\} \frac{2D_n}{\delta_{\uparrow}^2} dD_n \quad (53)$$

$$= \lambda_n \pi |\bar{\omega}_n|^{\frac{2}{\gamma}} \int_0^{\delta_\uparrow |\bar{\omega}_n|^{\frac{4}{\gamma}}} \mathbb{E} \left\{ J_0 \left(D_{1,n}^{-\frac{\gamma}{2}} H_n B^0 \right) - 1 \right\} 2D_{1,n} dD_{1,n} \quad (54)$$

Thus we have evaluated (13) as

$$\Phi_{\mathbf{Y}, \mathcal{S}_n}(\mathbf{w}) = e^{\lambda_n \pi |\bar{\omega}_n|^{\frac{2}{\gamma}} \int_0^{\delta_\uparrow |\bar{\omega}_n|^{\frac{4}{\gamma}}} \mathbb{E} \left\{ J_0 \left(D_{1,n}^{-\frac{\gamma}{2}} H_n B^0 \right) - 1 \right\} 2D_{1,n} dD_{1,n}}. \quad (55)$$

When $\delta_\uparrow \rightarrow \infty$, (55) can be written as

$$\Phi_{\mathbf{Y}, \mathcal{S}_n}(\mathbf{w}) = e^{\lambda_n \pi |\bar{\omega}_n|^{\frac{2}{\gamma}} \int_0^\infty \mathbb{E} \left\{ J_0 \left(D_{1,n}^{-\frac{\gamma}{2}} H_n B^0 \right) - 1 \right\} 2D_{1,n} dD_{1,n}} \quad (56)$$

$$= e^{-\sigma_n |\bar{\omega}_n|^\alpha} \quad (57)$$

where $\alpha = \frac{4}{\gamma}$, and $\sigma_n = \lambda_n \pi \int_0^\infty \mathbb{E} \left\{ 1 - J_0 \left(D_{1,n}^{-\frac{\gamma}{2}} H_n B^0 \right) \right\} 2D_{1,n} dD_{1,n}$. (57) is the characteristic function of a symmetric alpha stable random variable. If δ_\uparrow is finite, the characteristic function expression is not very useful, but converges rapidly as δ_\uparrow increases. Combining (9),(57), and (51), we arrive at the characteristic function of the Y as

$$\Phi_{\mathbf{Y}}(\mathbf{w}) = e^{-\sigma_0 \|\mathbf{w}\|^\alpha} \prod_{n=1}^N e^{-\sigma_n |\bar{\omega}_n|^\alpha}. \quad (58)$$

(58) is the characteristic function of random variable that is a mixture of independent and spherically isotropic symmetric alpha stable vectors. The dispersion parameters σ_0 and σ_n $n = 1, 2, \dots, N$ depend linearly on the intensities λ_0 and λ_n $n = 1, 2, \dots, N$, respectively. By setting λ_0 to 0, our model degenerates into spatially independent RFI, while setting λ_n to 0 for all $n = 1, 2, \dots, N$ causes isotropic RFI at the receiver.

In this scenario, the parameter σ_n ($n = 1, \dots, N$) is linearly dependent on the corresponding interferer density λ_n . If λ_n is very high, or in other words, the number of interferers becomes very large, the resulting interference is still distributed as a symmetric alpha stable random variable, albeit with a very high intensity. This is an interesting property in contrast to interference with guard zones, where interference statistics under a large value of λ_n are less impulsive in nature and start resembling the Gaussian distribution.

V. IMPACT OF SYSTEM MODEL ASSUMPTIONS ON INTERFERENCE STATISTICS

A. Interference statistics in general fading channel models

In developing our system model in Section III, we assumed a Rayleigh distributed fast fading channel between interfering sources and the multi-antenna receiver. While the Rayleigh distribution

is a reasonably accurate and frequently used model of fading channel amplitude, other distributions have also been widely used to characterize wireless channel amplitudes [31].

For unconstrained interferer location distribution, we do not require any assumptions on the channel amplitude distribution to derive RFI statistics. With constrained interferer locations, the Rayleigh distribution of the fading channel between interferers and the receiver was used to simplify the integral of a Bessel function in (30). Removing the Rayleigh distribution assumption would prevent this step in the proof. Since we are interested in the RFI amplitude tail statistics, and from Fourier analysis, the behavior of the characteristic function Φ in the neighborhood of $\|\mathbf{w}\| \rightarrow 0$ governs the tail probability of the random envelope [14]. We use the approximation [16]

$$\mathbb{E}_x \{J_0(x)\} = e^{-\mathbb{E}_x \{x\}} (1 + \Lambda(x)) \quad (59)$$

where $\Lambda(x)$ is a correction factor expressed as

$$\Lambda(x) = \sum_{m=2}^{\infty} \frac{(\mathbb{E}\{x^2\})^m}{2^{2m} m!} \mathbb{E}_1 F_1(-m; 1; \frac{x}{\mathbb{E}\{x\}}) \quad (60)$$

where ${}_1F_1(\cdot; \cdot; \cdot)$ is the confluent hypergeometric function of the first kind. It has been shown [14], [19] that as $x \rightarrow 0$, the slowest decaying term in $\Lambda(x)$ is of the order $\mathcal{O}(x^4)$, and we can write (59) as

$$\mathbb{E}_x \{J_0(x)\} = e^{-\mathbb{E}_x \{x\}}. \quad (61)$$

Using (61), we can simplify (26) as

$$\Psi_{\mathbf{Y}, \mathcal{S}_0}(\mathbf{w}) = \bar{K} \left(\mathbb{E} \left\{ \prod_{n=1}^N J_0 \left(|\bar{\omega}_n| D_0^{-\frac{\gamma}{2}} H_n^0 B^0 \right) \right\} - 1 \right) \quad (62)$$

$$= \bar{K} \left(\mathbb{E} \left\{ \prod_{n=1}^N \mathbb{E}_{H_n^0} \left\{ J_0 \left(|\bar{\omega}_n| D_0^{-\frac{\gamma}{2}} H_n^0 B^0 \right) \right\} \right\} - 1 \right) \quad (63)$$

$$\approx \bar{K} \left(\mathbb{E} \left\{ \prod_{n=1}^N e^{-\left\{ \left(|\bar{\omega}_n| D_0^{-\frac{\gamma}{2}} \mathbb{E}\{H_n^0\} B^0 \right)^2 \right\}} \right\} - 1 \right) \quad (64)$$

$$= \bar{K} \left(\mathbb{E}_{D_0, B^0} \left\{ e^{-\left\{ \left(\|\mathbf{w}\|^2 D_0^{-\frac{\gamma}{2}} \mathbb{E}\{H_n^0\} B^0 \right)^2 \right\}} \right\} - 1 \right) \quad (65)$$

Since we are interested in evaluating (26) primarily in the neighborhood of $\|\mathbf{w}\| \rightarrow 0$, we used (61) when stepping from (63) to (64). In stepping from (64) to (65), we used the assumption that the fading channel is *i.i.d.* across the receive antennas, therefore $\mathbb{E}\{(H_n^0)^2\}$ is independent of n . Since (65) has the same form as (34), the rest of the joint RFI statistics derivation continues from (34) as shown in Section IV-A, yielding joint statistics of the form given in (46).

B. Interference statistics in random interferer emissions

In deriving interferer statistics in the presence of guard zones, we assumed that the emission amplitude was constant in (38) in order to simplify the interference statistics into the form of a Middleton Class A distribution. Without making this assumption, (40) would be replaced by

$$\Psi_{\mathbf{Y}, \mathcal{S}_0}(\mathbf{w}) = \lambda \pi \delta_{\perp}^2 \eta_{\gamma} \mathbb{E}_{B^0} \left\{ e^{-\frac{\|\mathbf{w}\|^2 \delta_{\perp}^{-\gamma} \beta_{\gamma} \mathbb{E}\{H^{0^2}\} (B^0)^2}{4}} - 1 \right\} \quad (66)$$

As discussed in Section V-A, in order to accurately model tail probabilities, we are concerned with the region around $\|\mathbf{w}\| \rightarrow 0$. In this region, we can use the approximation $e^x \approx 1 + x$, to arrive at

$$\mathbb{E}_{B^0} \left\{ e^{-\frac{\|\mathbf{w}\|^2 \delta_{\perp}^{-\gamma} \beta_{\gamma} \mathbb{E}\{H^{0^2}\} (B^0)^2}{4}} - 1 \right\} \approx \mathbb{E} \left\{ \frac{-\|\mathbf{w}\|^2 \delta_{\perp}^{-\gamma} \beta_{\gamma} \mathbb{E}\{H^{0^2}\} (B^0)^2}{4} \right\} \quad (67)$$

$$= \frac{-\|\mathbf{w}\|^2 \delta_{\perp}^{-\gamma} \beta_{\gamma} \mathbb{E}\{H^{0^2}\} \mathbb{E}\{(B^0)^2\}}{4} \quad (68)$$

Again, by using the approximation $1 + x \approx e^x$, we can combine (66) and (68) to get

$$\Psi_{\mathbf{Y}, \mathcal{S}_0}(\mathbf{w}) \approx \lambda \pi \delta_{\perp}^2 \eta_{\gamma} \left(e^{\frac{-\|\mathbf{w}\|^2 \delta_{\perp}^{-\gamma} \beta_{\gamma} \mathbb{E}\{H^{0^2}\} \mathbb{E}\{(B^0)^2\}}{4}} - 1 \right) \quad (69)$$

which has the same form as (40). Thus, even if the interferer emission envelopes are randomly distributed, the interference statistics can be approximated using the Middleton Class A form, especially in the tail probability region. Note that when we derive RFI statistics in the absence of guard zones we make no assumptions regarding the interferer emission amplitude.

C. Interference statistics in spatially correlated wireless channel models

To derive the joint statistics of RFI in Sections IV-B and IV-A, we assume that the wireless fading channel between the interfering source and receiver is spatially independent and identically distributed across the multiple antennas in the receiver. This assumption may not be true if two antennas are close to each other. Spatial correlations in the wireless channel are routinely modeled when studying the performance of multi-antenna receivers [32], [33]. In this paper, we only study the impact of channel correlation on the joint interference statistics in the presence of guard zones. We start from (25), which shows that the joint log-characteristic function of RFI can be expressed as

$$\Psi_{\mathbf{Y}, \mathcal{S}_0}(\mathbf{w}) = \bar{K} \left(\mathbb{E} \left\{ \prod_{n=1}^N \sum_{m_n=0}^{\infty} j^{m_n} \epsilon_{m_n} J_{m_n} \left(|\bar{\omega}_n| D^{-\frac{\zeta}{2}} H_{n,0}^0 B_{n,0}^0 \right) \cos \left(m_n \left(\chi^0 + \Theta_n^0 + \xi_{\omega,n} \right) \right) \right\} - 1 \right). \quad (70)$$

In Section IV-B we used the assumption that the fast-fading channel phase is uncorrelated across receive antennas, to show that all terms with $m_n > 0$ are equal to zero, resulting in the simplified product of terms expression in (26). If there is phase correlation between receive antennas u and

ν , then the terms containing $\mathbb{E}\left\{\cos\left(k_u(\chi^0 + \Theta_u^0 + \xi_{\omega,u}) + k_\nu(\chi^0 + \Theta_\nu^0 + \xi_{\omega,\nu})\right)\right\}$ are not equal to zero for $k_u, k_\nu > 0$. However, assuming that the interferer emissions are uniformly distributed in phase χ^0 , only the terms with $k_\nu = -k_u$ and $k_u = k_\nu = 0$ are non-zero, and considering only these terms (70) reduces to

$$\Psi_{\mathbf{Y}, \mathcal{S}_0}(\mathbf{w}) = \bar{K} \times \mathbb{E} \left\{ \left(\prod_{\substack{n=1 \\ n \neq u, \nu}}^N J_0(|\bar{\omega}_n| D^{-\frac{\gamma}{2}} H_n^0 B^0) \right) \sum_{m=0}^{\infty} J_m(|\bar{\omega}_u| D^{-\frac{\gamma}{2}} H_u^0 B^0) J_m(|\bar{\omega}_\nu| D^{-\frac{\gamma}{2}} H_\nu^0 B^0) \cos(m(\Theta_u^0 - \Theta_\nu^0 + \xi_{\omega,u} - \xi_{\omega,\nu})) \right\} - 1. \quad (71)$$

By applying the following identity,

$$J_0\left(\sqrt{a^2 + b^2 - 2ab \cos(x)}\right) = \sum_{m=0}^{\infty} J_m(a) J_m(b) \epsilon_m \cos(mx) \quad (72)$$

(71) can be expressed as

$$\Psi_{\mathbf{Y}, \mathcal{S}_0}(\mathbf{w}) = \bar{K} \mathbb{E} \left\{ \left(\prod_{\substack{n=1 \\ n \neq u, \nu}}^N J_0(|\bar{\omega}_n| D^{-\frac{\gamma}{2}} H_n^0 B^0) \right) \times J_0\left(\sqrt{(|\bar{\omega}_u| D^{-\frac{\gamma}{2}} H_u^0 B^0)^2 + (|\bar{\omega}_\nu| D^{-\frac{\gamma}{2}} H_\nu^0 B^0)^2 - 2|\bar{\omega}_u| |\bar{\omega}_\nu| D^{-\gamma} H_u^0 H_\nu^0 (B^0)^2 \cos(\Theta_u^0 - \Theta_\nu^0 + \xi_{\omega,u} - \xi_{\omega,\nu})}\right) \right\} - 1. \quad (73)$$

We again use the approximation result provided in (59) to get

$$\begin{aligned} \Psi_{\mathbf{Y}, \mathcal{S}_0}(\mathbf{w}) &= \bar{K} \left(\mathbb{E} \left\{ e^{-D_0^{-\gamma} (B^0)^2 \sum_{n=1}^N (|\bar{\omega}_n|^2 \mathbb{E}\{(H_n^0)^2\}) - 2|\bar{\omega}_u| |\bar{\omega}_\nu| \mathbf{E}\{H_{u,0}^0 H_{\nu,0}^0\} \cos(\Theta_u^0 - \Theta_\nu^0 + \xi_{\omega,u} - \xi_{\omega,\nu})} \right\} - 1 \right) \\ &= \bar{K} \left(\mathbb{E} \left\{ e^{-D_0^{-\gamma} (B^0)^2 \sum_{n=1}^N (|\bar{\omega}_n|^2 \mathbb{E}\{(H_n^0)^2\})} e^{2D_0^{-\gamma} (B^0)^2 \omega_{u,I} \omega_{\nu,I} \mathbf{E}\{H_{u,0}^0 H_{\nu,0}^0 \cos(\Theta_{u,0} - \Theta_{\nu,0})\}} \right. \right. \\ &\quad \times e^{2D_0^{-\gamma} (B^0)^2 \omega_{u,Q} \omega_{\nu,Q} \mathbf{E}\{H_{u,0}^0 H_{\nu,0}^0 \cos(\Theta_{u,0} - \Theta_{\nu,0})\}} \times e^{2D_0^{-\gamma} (B^0)^2 \omega_{u,I} \omega_{\nu,Q} \mathbf{E}\{H_{u,0}^0 H_{\nu,0}^0 \sin(\Theta_{u,0} - \Theta_{\nu,0})\}} \\ &\quad \left. \left. \times e^{2D_0^{-\gamma} (B^0)^2 \omega_{u,Q} \omega_{\nu,I} \mathbf{E}\{H_{u,0}^0 H_{\nu,0}^0 \sin(\Theta_{u,0} - \Theta_{\nu,0})\}} \right\} - 1 \right). \quad (75) \end{aligned}$$

Note that in addition to the $|\bar{\omega}_n|^2$ terms, $\Psi_{\mathbf{Y}, \mathcal{S}_0}(\mathbf{w})$ contains non-zero terms with variables $2\omega_{u,R}\omega_{\nu,R}$, $2\omega_{u,R}\omega_{\nu,I}$, $2\omega_{u,I}\omega_{\nu,I}$, and $2\omega_{u,I}\omega_{\nu,R}$. These terms indicates sample level correlation in the sum RFI, for example the coefficient of the $2\omega_{u,R}\omega_{\nu,R}$ term is indicative of correlation between $Y_{u,R}$ and $Y_{\nu,R}$.

Analogous to the cross terms in multi-dimensional Gaussian distributions, this coefficient of the $2\omega_{u,R}\omega_{v,R}$ term is equal to $\mathbb{E}\{Y_{u,R}Y_{v,R}\}$. Thus we can now update our model to include correlation

$$\Phi_{\mathbf{Y}}(\mathbf{w}) = e^{A_0 \left(e^{-\frac{\mathbf{w}^T \mathbf{K}^{-1} \mathbf{w}}{2}} - 1 \right)} \times \prod_{n=1}^N e^{A_n \left(e^{-\frac{|\bar{\omega}_n|^2 \Omega_n}{2}} - 1 \right)}. \quad (76)$$

The probability distribution corresponding to the characteristic function in (45) can be written as

$$f(\mathbf{Y}) = \left\{ \prod_{n=1}^N \left\{ \sum_{m_n=1}^{\infty} \frac{e^{-A_n (A_n)^{m_n}}}{m_n!} e^{-\frac{|Y_n|^2}{\Omega_n}} \right\} \right\} \sum_{m_0=1}^{\infty} \frac{e^{-A_0 (A_0)^{m_0}}}{m_0!} e^{-\frac{\mathbf{y}^T \mathbf{K}^{-1} \mathbf{y}}{\Omega_0}} \quad (77)$$

where the matrix \mathbf{K} is a $2N \times 2N$ matrix. For all integers $u, v \in [1, N]$, the elements of \mathbf{K} are given as

$$K_{2u,2v} = \mathbb{E} \left\{ H_u^0 H_v^0 \cos(\Theta_u^0 - \Theta_v^0) \right\} \quad (78)$$

$$K_{2u+1,2v+1} = \mathbb{E} \left\{ H_u^0 H_v^0 \cos(\Theta_u^0 - \Theta_v^0) \right\} \quad (79)$$

$$K_{2u,2v+1} = \mathbb{E} \left\{ H_u^0 H_v^0 \sin(\Theta_u^0 - \Theta_v^0) \right\} \quad (80)$$

$$K_{2u+1,2v} = \mathbb{E} \left\{ H_u^0 H_v^0 \sin(\Theta_u^0 - \Theta_v^0) \right\} \quad (81)$$

$$K_{2u,2u} = \mathbb{E} \left\{ (H_u^0)^2 \right\} \quad (82)$$

$$K_{2u+1,2u+1} = \mathbb{E} \left\{ (H_u^0)^2 \right\}. \quad (83)$$

D. Interference statistics in randomly distributed pathloss exponents

In our system model, we assumed that the pathloss exponent is fixed across emissions from all possible interferers. However, many indoor wireless channel models account for variable pathloss exponents [34]. If we consider the pathloss exponent to be a random variable G with support \mathcal{G} and a discrete probability density $\mathbb{P}(G = \gamma_t) = p_t \quad \forall t = 1, \dots, |\mathcal{G}|$, we can write (4) as

$$Y_n = \sum_{t=0}^{|\mathcal{G}|} p_t \sum_{i_0 \in \mathcal{S}_0} B_{i_0}^0 D_{0,i_0}^{-\frac{\gamma_t}{2}} H_{n,i_0}^0 e^{j(\chi_{i_0}^0 + \Theta_{n,i_0}^0)} + \sum_{i \in \mathcal{S}_n} B_i^n D_{n,i}^{-\frac{\gamma_t}{2}} H_i^n e^{j(\chi_i^n + \Theta_i^n)}. \quad (84)$$

where each term in the outer summation is the sum interference from a Poisson field of interferers with pathloss exponent of γ_t . Assuming that the pathloss exponent is independent of the interferers, the Poisson field of interferers gets randomly thinned by probability p_t , resulting in another Poisson field with intensity λp_t . Thus, the total interference is the sum of interference from $|\mathcal{G}|$ independent fields of interferers. In the scenario where there are no guard zones around the receiver, the characteristic function of interference would represent the sum of many alpha stable random variables, which can be written as

$$\Phi_{\mathbf{Y}}(\mathbf{w}) = \prod_{t=1}^{\mathcal{P}} e^{-p_t \sigma_{0,\gamma_t} \|\mathbf{w}\|^{\frac{4}{\gamma_t}}} \prod_{n=1}^N e^{-p_t \sigma_{n,\gamma_t} |\bar{\omega}_n|^{\frac{4}{\gamma_t}}} \quad (85)$$

$$= e^{-E_G\{\sigma_{0,G}\|\mathbf{w}\|^{\frac{4}{\alpha}}\}} \prod_{n=1}^N e^{-E_G\{\sigma_{n,G}|\bar{\omega}_n|^{\frac{4}{\alpha}}\}}. \quad (86)$$

In (85), σ_{0,γ_t} is the same as σ_0 derived in (58) with indexing γ_t indicating its dependence on γ_t .

In the case where a guard zone exists around the receiver, the resulting interference is the sum of independent multi-dimensional Middleton Class A random variables, which exhibits the Gaussian mixture distribution. The characteristic function of interference from set \mathcal{S}_0 can be expressed by modifying (43) to write it as

$$\Psi_{\mathbf{Y},\mathcal{S}_0}(\mathbf{w}) = \prod_{t=1}^{\mathcal{P}} e^{p_t A_{0,\gamma_t} \left(e^{-\frac{\|\mathbf{w}\|^2 \Omega_{0,\gamma_t}}{2}} - 1 \right)} \quad (87)$$

$$= e^{\mathbb{E}_G\left\{ A_{0,G} \left(e^{-\frac{\|\mathbf{w}\|^2 \Omega_{0,G}}{2}} - 1 \right) \right\}}. \quad (88)$$

It may require some extra mathematical rigor to prove the same results when the pathloss exponent is a continuous random variable.

E. Discussions on remaining system model assumptions

The key assumptions that remain in our system model are:

Poisson point process distribution of interferer locations — The Poisson point process distribution of interferer locations has been shown to well model cellular networks, ad-hoc networks and uncoordinated radiative sources. Other point processes can also be used to model a variety of applications; for example, the clustered Poisson point process is a good interferer location distribution model for heterogeneous and two-tier networks [19].

Interferers visible to a subset of receive antennae — In this paper, we assumed interferers that were either observed by all receive antennas or by only a single receive antenna. This assumption can be extended to include interferers that are visible by only a subset of receiver antennas, giving rise to a possible $2^N - 1$ different sets of interferers for a N antenna receiver. Our statistical derivations are also amenable to incorporating such scenarios, as each set of interferers would result in RFI statistics that are statistically isotropic across the subset of receiver antennas observing the interferer set.

Neglecting inter-antenna spacing at the receiver — Using this assumption, we can employ a single random variable to denote the distance from a interferer in the set \mathcal{S}_0 to each receive antennas. In the case when $\delta_1 = 0$, and there is no inter-antenna spacing, we have shown that interference statistics exhibit spatial isotropy. If the inter-antenna spacing is asymptotically large, each antenna would observe interference from different interferers causing interference to be independent across

TABLE IV: Parameter values used in simulations

Parameter	Description	Value
λ_{tot}	Per-antenna total intensity of interferers	0.01
γ	Power path-loss exponent	4
\bar{B}	Mean amplitude of interferer emissions	1.0
δ_{\perp}	Radius of guard zone around receiver	1.5
$\mathbb{E}\{H^2\}$	Fast fading channel power	1.0

antennas. It intuitively follows that increasing inter-antenna spacing reduces the spatial dependence in the resulting interference statistics, which move from spatially isotropic to spatially independent. It may therefore be possible to apply our proposed continuum between isotropy and independence to approximate the statistics of interference in receivers with significantly separate antennas. Modeling joint statistics of RFI between separate antennas is beyond the scope of this paper and an avenue of future work.

In the presence of guard zones, antenna spacing may be ignored if the radius of the guard zone is much larger than the inter-antenna distances at the receiver. This is simply because the distance between any interferer and an antenna is larger than the guard zone radius, consequently antenna geometry will have minimal impact on the pathloss attenuation term in (1). In single antenna receivers, it has been shown that if an antenna is placed a small distance away from the center of the guard zone, the statistics of resulting interference are unchanged [19].

VI. SIMULATION RESULTS

To study the accuracy of our joint amplitude distribution model, we numerically simulate the random variable \mathbf{Y} as given in (5) and (6). \mathbf{Y} describes the observed RFI across a simulated multi-antenna receiver in a Poisson field of interferers. Our receiver uses $N = 3$ antennas and the interferers exclusive to each antenna are distributed with equal densities, i.e. $\lambda_1 = \lambda_2 = \lambda_3 = \lambda_e$. We choose λ_0 such that $\lambda_0 + \lambda_e = 0.01$, i.e. the density of total interferers observed by each antenna is the same, in order to normalize our data as the variance of interference observed at each antenna (proportional to $\lambda_0 + \lambda_e$) remains the same regardless of the value taken by λ_0 or λ_e . Table IV lists the values for the rest of the simulation parameters.

Figure 2 shows a scatter plot of the amplitude of simulated random RFI observed at two antennas over a span of 40 time samples using different values of λ_0 and λ_e . The horizontal axis denotes the

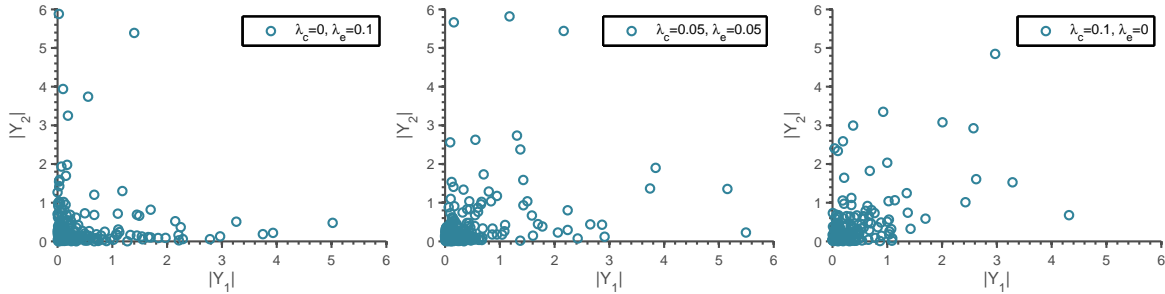


Fig. 2: Scatter plot of RFI amplitude observed at 2 receive antennas.

RFI amplitude at antenna 1 and the vertical axis denotes the RFI amplitude at antenna 2. As λ_0 increases, the RFI samples move towards the top left of the scatter plot area, indicating that impulsive events (samples with a large amplitude) occur in a spatially dependent manner, i.e., impulsive events at the two receive antennas occur with different strengths but at the same location in time.

To validate our amplitude distribution model, we use two metrics: (1) the Kullback-Liebler (KL) divergence between numerically simulated interference amplitude distribution and our proposed amplitude distribution; and (2) the tail probabilities of the numerically simulated and our proposed amplitude distribution. Although KL divergence is not strictly a distance metric, it is often used to compare probability density distributions and can be computed efficiently. Low KL divergence between two density distributions implies high similarity between the density functions. Figure 3 shows the KL divergence between the numerically simulated distribution of interference in the presence of guard zones and our proposed multi-variate Class A model. We also show the KL divergence between the numerically simulated distribution and the isotropic and independent-only multi-variate distributions given in Table II as MCA.III and MCA.I, respectively. The KL divergence between the numerically simulated RFI amplitude distribution and our proposed models is lowest across all values of λ_0 , indicating that our proposed distribution is able to well capture partial spatial dependence in interference. The KL divergence between simulated RFI and multi-variate Gaussian distribution of equal variance is also shown in Figure 3, and it is very large owing to the fact that the Gaussian distribution cannot accurately model impulsiveness in simulated RFI.

Next, we compare the tail probabilities of the numerically simulated distribution and our proposed distribution models. The tail probability is the complementary cumulative distribution function of a random variable and in performance analysis of communication systems, the tail probability of interference is related to the outage performance of receivers. Given a threshold τ , we define tail

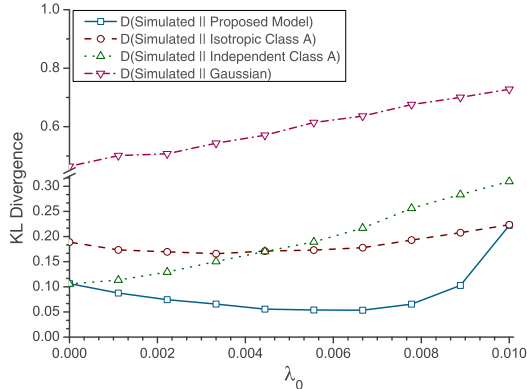


Fig. 3: Estimated KL divergence between simulated RFI distribution and proposed model vs. λ_0 ($\lambda_e = 0.01 - \lambda_0$), where a lower KL divergence means a better fit. $D(P||Q)$ denotes the KL divergence between distributions P and Q . KL divergence is also calculated between the simulated RFI distribution and models MCA.I (Independent Class A) and MCA.III (Isotropic Class A) from Table II.

probability as $\mathbb{P}(|Y_1| > \tau, \dots, |Y_N| > \tau)$. Figures 4 and 5 shows a comparison of the tail probabilities of the numerically simulated distribution, our proposed distribution, and the Gaussian distribution for interference with and without guard zones, respectively. The tail probability of the multi-dimensional Middleton Class A distribution can be evaluated as a mixture of Gaussian tail probabilities, and the approximate tail probability of the symmetric alpha stable distribution is given in [15]. The tail probabilities of our proposed distributions match closely to simulated interference, while the Gaussian distribution is clearly unable to capture the large tail probabilities of impulsive interference.

We also employ KL divergence to study the impact of different channel models on the resulting spatial distribution of RFI. We use three common stochastic fading channel models [31]. When the dominant propagation path is line-of-sight, a Rician model is commonly used. Otherwise, a Rayleigh or Nakagami model is commonly used. Table V defines the three distributions, and the parameters values used in simulation. The system parameter values are chosen from Table IV. Figure 6 shows that the KL divergence with Rayleigh fading channel model is the lowest, which is to be expected. The KL divergence increases slightly upon changing the channel model, indicating that the approximation used in (59) is close to its true value.

Finally, we simulate correlated fading channels to test whether our model correctly accounts for spatial correlation. We simulate correlation between the in-phase components of the channel between an interferer and the two receive antennas. The Pearson product moment correlation coefficient (PMCC) [35] between these two random variables is chosen as 0.3. Using (78), the PMCC

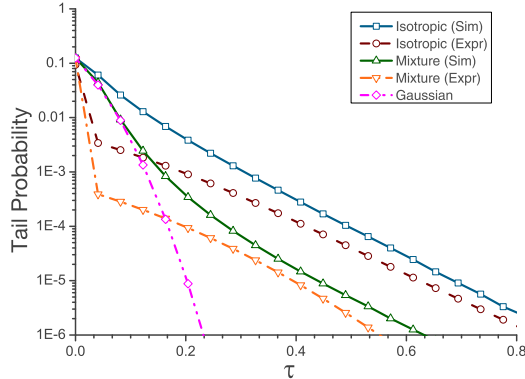


Fig. 4: Tail probability vs. threshold τ for interference in the presence of guard zones. The tail probability is compared between the numerically simulated interference (“Sim”) and the tail of our proposed multi-variate Middleton Class A distribution (“Expr”). The tail probabilities are generated for isotropic interference ($\lambda_0 = 0.01, \lambda_e = 0.0$) and a mixture of isotropic and independent interference ($\lambda_0 = 0.001, \lambda_e = 0.009$). Remaining parameter values are given in Table IV.

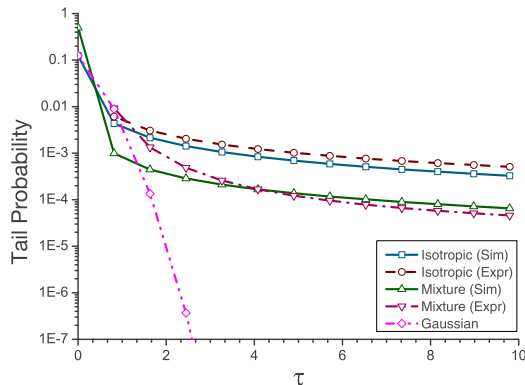


Fig. 5: Tail probability vs. threshold τ for interference in the absence of guard zones ($\delta_1 = 0$). The tail probability is compared between the numerically simulated interference (“Sim”) and the tail of the multi-variate symmetric alpha stable distribution (“Expr”). The tail probabilities are generated for isotropic interference ($\lambda_0 = 0.01, \lambda_e = 0.0$) and a mixture of isotropic and independent interference ($\lambda_0 = 0.001, \lambda_e = 0.009$). Remaining parameter values are given in Table IV.

between the in-phase components of the two receive antennas has a predicted value of $\frac{0.3\lambda_0}{\lambda_0 + \lambda_e}$. Figure 7 shows that the empirically estimated value of the PMCC matches our prediction quite accurately.

VII. CONCLUSIONS

In this paper, we propose a statistical-physical framework for modeling RFI observed by a multi-antenna receiver surrounded by interference causing emitters. Our framework incorporates random distribution of interferer locations in two-dimensional space around the receiver with an optional

TABLE V: Commonly used fast fading channel models [31] used in Figure 6.

Channel Model	Parameters
Rayleigh fading: $f(x) = \frac{x}{\sigma^2} e^{-\frac{x^2}{2\sigma^2}}$	$\sigma = 1$
Rician fading: $f(x) = \frac{2(K+1)x}{\Omega} e^{-K - \frac{(K+1)x^2}{\Omega}} I_0\left(2\sqrt{\frac{K(K+1)}{\Omega}}x\right)$	$K = 2, \Omega = 1$
Nakagami fading: $f(x) = \frac{2\mu^\mu}{\Gamma(\mu)\omega^\mu} x^{2\mu-1} e^{-\frac{\mu}{\omega}x^2}$	$\mu = 0.5, \omega = 1$

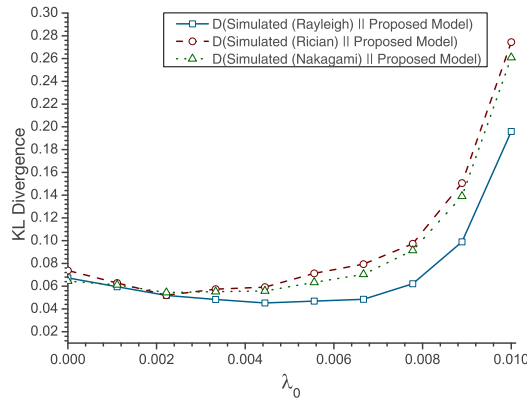


Fig. 6: Estimated KL divergence between simulated RFI distribution and proposed model vs. λ_0 , where a lower KL divergence means a better fit, using different fast fading channel models. The density function corresponding to each channel model is provided in Table V. $\lambda_e = 0.01 - \lambda_0$, and remaining parameters are given in Table IV. $D(P||Q)$ denotes KL divergence between distributions P and Q .

interferer-free guard zone, and physical mechanisms describing the generation and propagation of interference through the wireless medium, such as fast fading and pathloss attenuation. Our framework also incorporates partial statistical dependence of RFI across the receive antennas and captures a continuum between spatially independent and spatially isotropic interference.

Using our proposed framework, we derive the joint statistics of interference observed across a multi-antenna receiver, with the resulting amplitude distribution modeling both spatially isotropic and spatially independent observations of RFI as special cases. Depending on the region within which interferers are distributed, the interference statistics can be modeled using the Middleton Class A or the symmetric alpha stable distribution. Some of these distributions find use in designing interference mitigation algorithms or analyzing communication performance of receivers in the presence of interference. By providing a link between network models and interference distribution, our proposed models can better inform such analysis. This leads to the design of robust receivers that are better suited to operate in the presence of interference in different network environments.

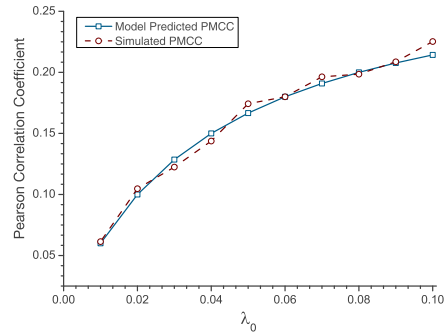


Fig. 7: Estimated Pearson Product Moment Correlation Coefficient (PMCC) vs. λ_0 . $\lambda_e = 0.04$ and other parameter values are given in Table IV.

REFERENCES

- [1] J. Shi, A. Bettner, G. Chinn, K. Slattery, and X. Dong, "A study of platform EMI from LCD panels - impact on wireless, root causes and mitigation methods," in *IEEE International Symposium on Electromagnetic Compatibility*, vol. 3, Portland, Oregon, Aug. 2006, pp. 626–631.
- [2] D. Lopez-Perez, A. Juttner, and J. Zhang, "Dynamic frequency planning versus frequency reuse schemes in OFDMA networks," in *IEEE Vehicular Technology Conference*, Apr. 2009, pp. 1–5.
- [3] A. Hasan and J. G. Andrews, "The guard zone in wireless *ad hoc* networks," *IEEE Transactions on Wireless Communications*, vol. 4, no. 3, pp. 897–906, Mar. 2007.
- [4] J. M. Peha, "Wireless communications and coexistence for smart environments," *IEEE Transactions on Personal Communications*, vol. 7, no. 5, pp. 66–68, May 2000.
- [5] J. G. Andrews, "Interference cancellation for cellular systems: A contemporary overview," *IEEE Wireless Communications Magazine*, vol. 12, no. 2, pp. 19–29, Apr. 2005.
- [6] V. R. Cadambe and S. A. Jafar, "Interference alignment and spatial degrees of freedom for the K user interference channel," in *Proc. IEEE International Conference on Communications*, May 2008, pp. 971–975.
- [7] M. Senst and G. Ascheid, "Optimal output back-off in OFDM systems with nonlinear power amplifiers," in *Proc. IEEE International Conference on Communications*, Jun. 2009, pp. 1–6.
- [8] C. Chan-Byoung, K. Sang-hyun, and R. W. Heath, "Linear network coordinated beamforming for cell-boundary users," in *Proc. IEEE Workshop on Signal Processing Advances in Wireless Communications*, Jun. 2009, pp. 534–538.
- [9] A. Chopra, K. Gulati, B. L. Evans, K. R. Tinsley, and C. Sreerama, "Performance bounds of MIMO receivers in the presence of radio frequency interference," in *Proc. IEEE International Conference on Acoustics, Speech, and Signal Processing*, Taipei, Taiwan, Apr. 19–24 2009.
- [10] M. Nassar, K. Gulati, A. K. Sujeeth, N. Aghasadeghi, B. L. Evans, and K. R. Tinsley, "Mitigating near-field interference in laptop embedded wireless transceivers," in *Proc. IEEE International Conference on Acoustics, Speech and Signal Processing*, May 2008, pp. 1405–1408.
- [11] A. Rabbachin, T. Q. S. Quek, H. Shin, and M. Z. Win, "Cognitive network interference," *IEEE Transactions on Selected Areas in Communications*, vol. 29, no. 2, pp. 480–493, Feb. 2011.
- [12] E. Biglieri, R. Calderbank, A. Constantinides, A. Goldsmith, A. Paulraj, and H. V. Poor, *MIMO Wireless Communications*, 2007.
- [13] A. Goldsmith, *Wireless Communications*. Cambridge University Press, 2005.

- [14] D. Middleton, "Non-Gaussian noise models in signal processing for telecommunications: New methods and results for class A and class B noise models," *IEEE Transactions on Information Theory*, vol. 45, no. 4, pp. 1129–1149, May 1999.
- [15] G. Samorodnitsky and M. S. Taqqu, *Stable Non-Gaussian Random Processes: Stochastic Models with Infinite Variance*. Chapman and Hall, New York, 1994.
- [16] D. Middleton, "Statistical–physical models of man–made and natural radio noise part II: First order probability models of the envelope and phase," U.S. Department of Commerce, Office of Telecommunications, Tech. Rep., Apr. 1976.
- [17] E. S. Sousa, "Performance of a spread spectrum packet radio network link in a Poisson field of interferers," *IEEE Transactions on Information Theory*, vol. 38, no. 6, pp. 1743–1754, Nov. 1992.
- [18] J. Ilow and D. Hatzinakos, "Analytic alpha-stable noise modeling in a Poisson field of interferers or scatterers," *IEEE Transactions on Signal Processing*, vol. 46, no. 6, pp. 1601–1611, Jun. 1998.
- [19] K. Gulati, B. Evans, J. Andrews, and K. Tinsley, "Statistics of co-channel interference in a field of Poisson and Poisson-Poisson clustered interferers," *IEEE Transactions on Signal Processing*, vol. 58, Dec. 2010.
- [20] S. M. Zabin and H. V. Poor, "Efficient estimation of class A noise parameters via the EM algorithm," *IEEE Transactions on Information Theory*, vol. 37, no. 1, pp. 60–72, Jan 1991.
- [21] J. P. Nolan, "Multivariate stable densities and distribution functions: General and elliptical case," in *Deutsche Bundesbank's Annual Fall Conference*, 2005.
- [22] P. A. Delaney, "Signal detection in multivariate Class-A interference," *IEEE Transactions on Communications*, vol. 43, no. 4, Feb. 1995.
- [23] P. Gao and C. Tepedelenioglu, "Space-time coding over fading channels with impulsive noise," *IEEE Transactions on Wireless Communications*, vol. 6, no. 1, pp. 220–229, Jan. 2007.
- [24] Y. Chen and R. S. Blum, "Efficient algorithms for sequence detection in non-Gaussian noise with intersymbol interference," *IEEE Transactions on Communications*, vol. 48, no. 8, pp. 1249–1252, Aug. 2000.
- [25] K. F. McDonald and R. S. Blum, "A statistical and physical mechanisms-based interference and noise model for array observations," *IEEE Transactions on Signal Processing*, vol. 48, pp. 2044–2056, July 2000.
- [26] K. Gulati, A. Chopra, R. W. Heath, B. L. Evans, K. R. Tinsley, and X. E. Lin, "MIMO receiver design in the presence of radio frequency interference," in *Proc. IEEE Global Telecommunications Conference*, Dec. 2008, pp. 1–5.
- [27] X. Yang and A. Petropulu, "Co-channel interference modeling and analysis in a Poisson field of interferers in wireless communications," *IEEE Transactions on Signal Processing*, vol. 51, Jan. 2003.
- [28] M. J. Dumbrell and I. J. Rees, "Sectorized cellular radio base station antenna," U.S. Patent 5 742 911, 1998.
- [29] T. S. Lee and Z. S. Lee, "A sectorized beamspace adaptive diversity combiner for multipath environments," *IEEE Transactions on Vehicular Technology*, vol. 48, no. 5, pp. 1503–1510, 1999.
- [30] D. Middleton, "Procedures for determining the properties of the first-order canonical models of class A and class B electromagnetic interference," *IEEE Transactions on Electromagnetic Compatibility*, vol. 22, pp. 190–208, Aug. 1979.
- [31] M. K. Simon and M.-S. Alouini, *Digital Communications Over Fading Channels*, 2nd ed.
- [32] L. Schumacher, K. Pedersen, and P. Mogensen, "From antenna spacings to theoretical capacities - guidelines for simulating MIMO systems," in *IEEE International Symposium on Personal, Indoor and Mobile Radio Communications*, vol. 2, Sept. 2002, pp. 587 – 592.
- [33] J. Luo, J. R. Zeidler, and S. McLaughlin, "Performance analysis of compact antenna arrays with maximal ratio combining in correlated Nakagami fading channels," *IEEE Transactions on Vehicular Technology*, vol. 50, pp. 267–277, Jan. 2001.
- [34] A. Borrelli, C. Monti, M. Vari, and F. Mazzenga, "Channel models for IEEE 802.11b indoor system design," *IEEE International Conference on Communications*, vol. 6, pp. 3701–3705, 2004.
- [35] J. L. Rodgers and W. A. Nicewander, "Thirteen ways to look at the correlation coefficient," *The American Statistician*, vol. 42, no. 1, Feb. 1988.